Nanowire Synthesis and Characterization:

Erbium Chloride Silicate and Two Segment CdS-CdSe Nanowires and Belts

by

Sunay Turkdogan

A Thesis Presented in Partial Fulfillment
of the Requirements for the Degree
Master of Science

Approved April 2012 by the
Graduate Supervisory Committee:

Cun-Zheng Ning, Chair
Meng Tao
Hongbin Yu

ARIZONA STATE UNIVERSITY

May 2012

ABSTRACT

In this work, I worked on the synthesis and characterization of nanowires and belts, grown using different materials, in Chemical Vapor Deposition (CVD) system with catalytic growth method. Through this thesis, I utilized the Photoluminescence (PL), Secondary Electron Microscopy (SEM), Energy Dispersive Spectroscopy (EDS) and X-ray diffraction (XRD) analyses to find out the properties of Erbium Chloride Silicate (ECS) and two segment CdS-CdSe samples.

In the first part of my research, growth of very new material, Erbium Chloride Silicate (ECS), in form of core/shell Si/ECS and pure ECS nanowires, was demonstrated. This new material has very fascinating properties for new Si based photonic devices. The Erbium density in those nanowires is $1.6 \times 10^{22} cm^{-3}$ which is very high value compared to the other Erbium doped materials. It was shown that the luminescence peaks of ECS nanowires are very sharp and stronger than their counterparts. Furthermore, both PL and XRD peaks get sharper and stronger as growth temperature increases and this shows that crystalline quality of ECS nanowires gets better with higher temperature.

In the second part, I did a very detail research for growing two segment axial nanowires or radial belts and report that the structure type mostly depends on the growth temperature. Since our final step is to create white light LEDs using single axial nanowires which have three different regions grown with distinct materials and give red, green and blue colors simultaneously, we worked on growing CdS-CdSe nanowires or belts for the first step of our aim. Those

products were successfully grown and they gave two luminescence peaks with maximum 160 nm wavelength separation depending on the growth conditions. It was observed that products become more likely belt once the substrate temperature increases. Also, dominance between VLS and VS is very critical to determine the shape of the products and the substitution of CdS by CdSe is very effective; hence, CdSe growth time should be chosen accordingly. However, it was shown two segmented products can be synthesized by picking the right conditions and with very careful analyses. We also demonstrated that simultaneous two colors lasing from a single segmented belt structures is possible with strong enough-pumping-power.

DEDICATION

This thesis is dedicated to my family and especially my little son, Tan, and my daughter, Ece.

Without them, this thesis would not have been possible.

ACKNOWLEDGMENTS

TABLE OF CONTENTS

LIST OF TABLES

LIST OF FIGURES

Chapter 1

INTRODUCTION

1.1 Overview of Nanotechnology

After Richard Feynman gave a talk entitled "There is a plenty of room at the bottom", in 1959, he got the scientific world thinking small. As a matter of fact, he implied the nanotechnology in this talk, but Norio Toniguchi first introduced the term of Nanotechnology in his paper in 1974. His idea for nanotechnology was based on scaling down the existing technology to the next level by using top-down approach. On the other hand, K. Eric Drexler first introduced the bottom-up term in his book in 1986. Since those times, Nanotechnology has been attracted many interests to work on this new area. In recent years, scientists from a number of scientific disciplines including electrical engineering, mechanical engineering, physics, chemistry, material science and biology, and many others have shown considerable efforts to realize it`s unique potential.

In general, Nanotechnology refers to anything much smaller than human hair. If we think that human hair is about 60 μm ($60x10^{-6}m$) in diameter, we can imagine how small it is. In another word, one nanometer is three to six individual atoms in length. Although it is much smaller than any object we encounter in our life, it is larger than the scale of atoms and molecules. Thus, Richard Feynman said "There is a plenty of room at the bottom" for further miniaturization. Nanometer scale is impossible to be seen with naked eye even with some optical microscopes. There must be very capable and powerful devices to go down to that

1

scale. Here, one question comes up "Why scientists try to play with this tiny structure that requires very capable machines to see them." The answer is very simple and as the following; small devices are always faster than other bulk devices and due to their small size, they are lighter and can get into small spaces. Other very important reasons are that they are cheaper and more energy efficient compared to other technologies. Furthermore, small size brings different properties that can be used to create devices not built before.

In nanotechnology world, there are two terms 'top-down' and 'bottom-up'. These two methods employ different techniques to create complex structures, architectures and devices. The top-down method is quite mature technique that has been proven and used by semiconductor electronic industry for many years. The industry made integrated circuits smaller and smaller by exploiting the top-down approach. This method is basically same with what sculptors do. The technique starts with big piece of substrates, and etching and depositing layers by using different lithography techniques follow each other to fabricate structures which have low dimension. For 30 year, we have seen a huge shrinking on the device dimension and it keeps shrinking to about to atomic size. However, due to lack of new techniques and some limits of the current techniques, it is not possible to scale down to the atomic size by using top-down approach. In 2011, Intel announced that they will produce new 3D chips employing top-down approach to build 22 nm transistors and that will be the smallest size done via top-down approach.

On the other hand, bottom-up approach is completely different from top-down approach. By using this technique, we can overcome the limit of top-down approach which means that we can build devices containing just a few atoms or molecules. This technique is more like assembling sculpture from very tiny row material. Bottom-up technique is completely opposite of top-down approach because we use a big piece of material to obtain the small device, but for this case, we use very tiny elements such as atoms to build a new device. It is obvious that this technique will pave the way for new unique devices; however, in order to make mass production feasible, lots of effort should be performed by scientist to find very effective assembly techniques. The most impressive milestone for bottom-up approach was demonstrated by IBM in 1989, and they spelled out the letter "IBM" by manipulating 35 individual xenon atoms. On the other hand, some methods such as Langmuir Blodgett have been found to align the nanowires and nanostructure by compressing the surface of the solution [35]. By this way nanostructures can be transferred to the substrate to build new devices. However, scientists must be conducted a number of research to make them feasible for mass production. So far, there has been no any technique used in mass production to assemble Nano-structures, but in the near future, this can be accomplished because many scientists and engineers are currently working on this new technology. In this thesis, we will mostly concentrate on the bottom-up approach and it`s different growth techniques to synthesis nanowires.

1.2 History of Nanowires

The history of nanowire growth was actually started with the vapor-liquid –solid growth mechanism and the equation:

$$R\min = \frac{2Vl}{RT\ln(s)}\sigma\text{lv}$$

was written by R.S. Wagner for vapor–liquid-solid whisker growth in 1964 [1]. This equation gives the idea to find minimum whisker radius by using Vl-the molar volume of the metal droplet, σlv-the liquid vapor surface, and s-the degree of super saturation of the vapor. First, scientist at Hitachi utilized this technique and applied to grow III-V nanowhiskers in the early 1990s. At that time, this group achieved the positional and orientational control of nanowhiskers. As well as they also grew the first p-n junction based on nanowhiskers. After that time, mid 1990s, other research groups also started to involve to this area. A new growth technique which is called solid –liquid-solid process was proposed by William Buhro's group at Washington University. During that time, Charles Lieber group at Harvard University also started to work on the area of inorganic nanorods. Those are the first research groups that initiated the new research area of the today`s enchanting technology. In the late 1990s, semiconductor nanowires were become very impressive research area and expanded very rapidly in the nanoscience world. After that time, many research groups started to work on the semiconductor nanowires and their device applications. This huge interest in semiconductor nanowires and their applications can be seen from the pie plot (Figure 1.1) which represents the increase of number of nanowire related paper

with respect to years. It is very obvious that the number of published paper is being increased exponentially with years. This is a very significant sign to show how important this area is.
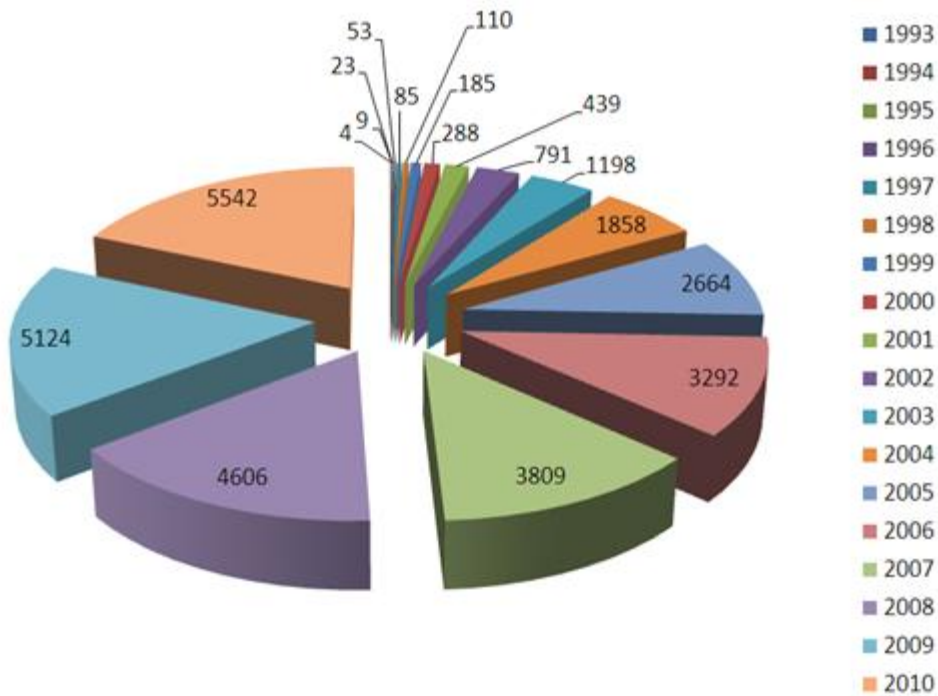
Figure 1.1 Number of nanowire related published paper with respect to year from 1993 through 2010. Colors indicate the year and numbers show the number of published paper in the particular year. Years increase clockwise. (Source: ISI Web of Knowledge)

1.3 Why Nanowires?

In the last paragraph, we said that the number of published paper increases exponentially, but we did not express why. The answer will be explained through this passage. Since the microelectronic technology is about to reach the bandwidth limit, different technologies have been started to study on more intensively, and nanowires seem one of the most important candidates for new photonic device technology, which will take the place of conventional electronic technology, due to their unique electrical and optical characteristics. Semiconductor nanowires have quasi-one dimensional structures with typically 10-300nm in diameter and several microns in length. In the literature, if wires have large aspect ratio (length / diameter > 20), they are called nanowires otherwise called nanorod. Since such a small size structure is under the limit of size for defect formation, it allows growing defect-free products. Nanowires have very unique properties that are not seen in any bulk material. This is because electrons in nanowires are quantum confined literally and hence occupy energy levels which are different than bulk-3D materials. In figure 1.2, the differences among structures of different dimensionality can be seen in terms of the density of states.

Nanowires are generally made of IV, III-V and II-VI semiconductor materials and they can be epitaxly grown without using expensive lithography techniques. Nanowires can exist in the air and thus the contrast of the refractive indices between nanowires (n~3.5) and air (n~1) is much higher than the contrast on the standard waveguides such as GaAs/AlGaAs [33]. Due to this fact, nanowires are good candidates for nano-lasers and waveguides because light can
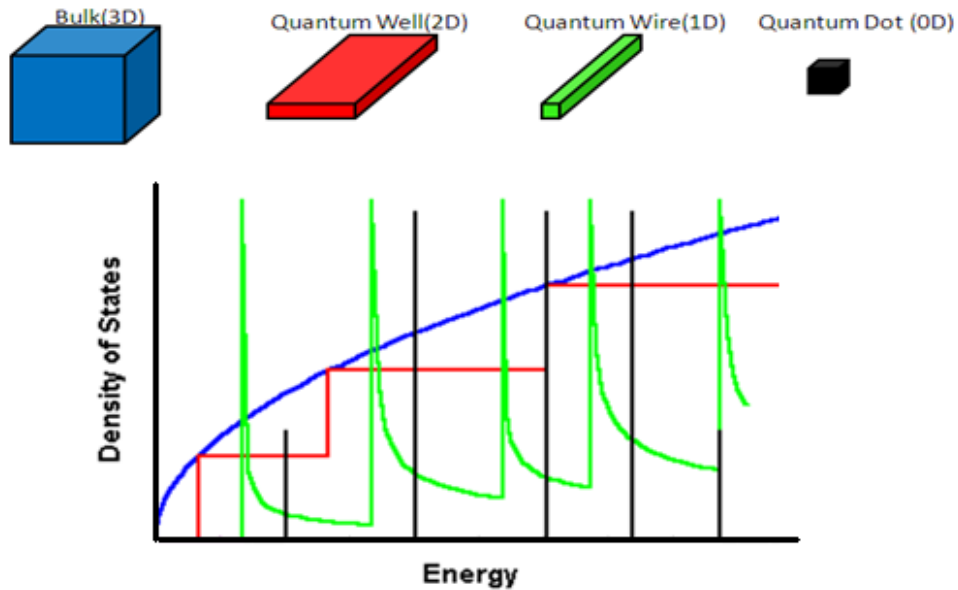
Figure 1.2 Density of states for bulk (3D blue), quantum well (2D red), quantum wire (1D green) and quantum Dot (0D black)

be well confined in the cavity. Another important feature of nanowires is that they can be grown by using widely available bandgap materials. That is why it is a good candidate for many device applications because having widely bandgap material is tough with planar epitaxial film growth, as well as nanowire growth shows much tolerance to lattice mismatch than planar epitaxial film growth. Furthermore, nanowires can be grown on any crystal or amorphous substrate and this offers a number of wavelength variations by alloying different semiconductors. This cannot be done with epitaxial film growth due to lattice mismatch problem. In addition to those features, nanowires are also considered as a Fabry-Perot cavity which is very important for Laser devices. In order to exploit their unique properties, scientists and engineers have built and have been creating different sort of devices such as solar cells, lasers, LEDs, field effect transistors, waveguides, and biological sensors, and many others.

Chapter 2

NANOWIRE GROWTH

2.1 Synthesis of Nanowires

After people realized the unique properties of nanowires, a number of groups started to find out different growth mechanisms for growing better nanowires in terms of optical, electrical and crystalline qualities. Although there have been a few mechanisms such as vapor-solid (VS), fluid liquid solid (FLS), solution liquid solid (SLS) and vapor liquid solid (VLS) to grow nanowires, VLS mechanism involves to synthesis of semiconductor nanowires in most cases and in this study as well. For this growth mechanism, metal nanoclusters are used as catalyst to initiate one dimensional growth. However, it does not mean that semiconductor nanowires cannot be grown without pre deposited metal catalyst. There are some cases which do not require pre deposited metal catalyst because one of the source materials can form metal droplets and act as catalyst. Catalyst is a very important step for 1-D growth because without them, we cannot grow nanowires or it takes forever to grow 1-D structure because thin film deposition dominates in case of absence of catalyst. It can be thought like enzyme in human body, and if there is no enough enzyme in the body, foods cannot be digested or this process takes very long time. This basically explains how important the usage of catalyst is. For nanowire case, fundamentally, metal nanoclusters dissolve one of the precursors from vapor phase to form a liquid alloy. Since the source materials are continuously supplied during the growth, this liquid alloys become supersaturated and at some point, nucleation occurs to create liquid solid

8

interface. Incoming vapor from source materials maintain the crystallization at this initial liquid-solid interface and leads to the highly anisotropic growth. As long as this growth conditions are kept, axial growth rate dominates the radial coating rate, and we grow long nanowires. However, in some cases, we need to alter the growth conditions to have coating layers on the nanowires. This will be studied in the next section.

Since Si nanowires with gold catalyst were studied more extensively, we will explain the process by utilizing this nanowire structure. First of all, in order to get nanowires, we need to have liquid droplets which absorb the source materials to initiate the growth of nanowires. However, as we know that the melting point for gold is 1064 C and it is 1414 C for Silicon. In order to have them in liquid phase, we need to heat them to very high temperature which is not desirable for semiconductor industry because for example; the temperature for conventional silicon technology is around 550 C – 600 C. However, due to the nature, we can make these droplets liquid by alloying them with any source material which can be soluble in the particular metal cluster. The minimum temperature used to make this alloy liquid is called Eutectic temperature.
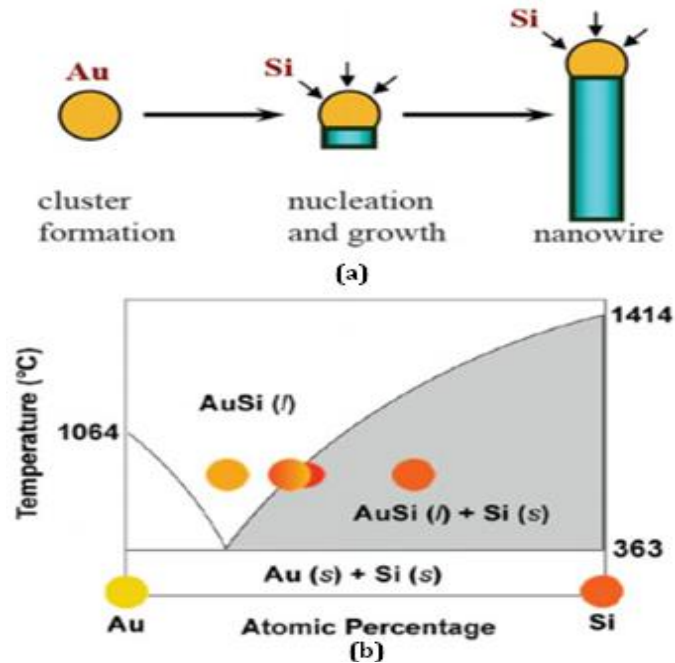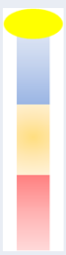
Figure 2.1 Sequence of Si nanowire growth (a) and binary phase diagram for Au and Si (b) [14]

As we can see from the binary phase diagram (figure 2.1), when metal catalyst is alloyed with Silicon, Gold nanoclusters form liquid droplets with Silicon at some point which is lower than the melting point of the Au and Si. Once the temperature is higher than eutectic temperature which is 370 C in this case, these alloyed droplets remain in the liquid state. As long as we supply source vapor, these droplets are saturated with incoming vapor. When the nanoclusters become supersaturated with a precursor, Silicon in this case, a nucleation event occurs and it produces solid-liquid interface ($AuSi_{(l)} + Si_{(s)}$) and subsequent solid growth occurs at this initial interface. In order to grow 1D structure, it is necessary to keep the nucleation on this initial interface and the nanodroplets should be in the liquid state otherwise we cannot grow 1D structure.

2.2 Nanowire Heterostructures

VLS mechanism gives us an opportunity to grow heterostructures at the individual device level by picking the appropriate fashion. This is not possible with the other growth techniques such as solution based liquid-solid growth. Therefore we can grow axial nanowires in which different composition materials have almost the same diameter and radial heterostructures in which there is a core/shell or core/multi shell structure by employing VLS and VS mechanisms. Recently, considerable efforts have been showed to grow axial and radial heterostructures. These types of structures were intensively studied and demonstrated by using VLS-CVD systems and those are summarized in table 2.1. In next paragraphs, we will go into the detail to understand how we grow radial or axial nanowires.

Table 2.1 Semiconductor Nanowire Heterostructures

	Group IV	Group III/V	Group II/VI
Radial NW Heterostructures	i-Si/p-Si Si/SiO2 Ge/Si Si/Ge Si/Ge/Si i-Si/SiO2/p-Si p-Si/i-Ge/SiO2/p-Ge	GaN/AlN/AlGaN n-GaN/InGaN/p-GaN n-GaN/InGaN/p-AlGaN/p-GaN n-GaN/InGaN MQW/p-AlGaN/p-GaN	CdS/CdSe
Axial NW Heterostructures	n-Si/p-Si n-Si/i-Si/p-Si Si/NiSi Si/Ge Si/GaP Si/GaAs	n-InP/p-InP GaAs/GaP InAs/GaAs InP/GaP InAs/InP	CdS/CdSe CdSe/CdS/ZnS

11

2.2.1 Axial Nanowires

Axial nanowire growth basically relies on the reaction of different source materials with the same metal catalyst. A very important requirement for the axial nanowire growth is nanoclusters catalyst should be suitable for growing two different components under similar conditions. Thus we need to pick the most appropriate metal clusters to use as a catalyst. According Duan et. al, gold is found the most appropriate nanoclusters to initiate axial nanowire growth. However, it has still some drawbacks and those problems will be studied in the next sections.

As a matter of fact, the mechanism to grow axial nanowires is very simple and the sequence can be seen in Figure 2.2. First of all, the growth starts as same as homogenous nanowire growth and after a period of time, we need to switch the source material with another one which is wanted to be as an extension of the first grown part. However, during the switching process, we most likely have a transition region on the nanowire because metal catalyst acts as a container and it can hold some material and supplies them until all the previous source is used up inside the catalyst. Although this is not a big issue in general, it can be a problem for some device applications. However, this can be solved by using solid catalyst or using different material than sources to supersaturate the metal catalyst. During the entire process, vapor-liquid-solid mechanism should dominate; otherwise we can get some deposition on the nanowires surface instead of getting the second segment on the same nanowire and it leads to have 2D growth which is desired

for radial nanowire growth. We will study this kind of nanowires growth in the next passage.

2.2.2 Radial Nanowires

Unlike axial nanowires in which different composition can be obtained by introducing the alternative vapor which reacts with the same metal catalyst, radial heterostructures can be grown by favoring growth for vapor-solid mechanism after the initial core layer growth synthesized via vapor-liquid-solid. This growth system is much different and tougher to perform than the system used for growing axial heterostructures. However, it can be applied very efficiently by picking the right system configurations and steps. Radial heterostructures offer better optical and electrical properties compared to the single composition nanowires. In order to grow good nanowires in terms of optical quality, surface passivation is required because surface area for 1D structure is very large and dangling bonds on the surface degrades the optical quality of the nanowires. If we grow around 10 nm shell layer on top of the nanowires, we can eliminate most of the effects caused by dangling bonds. By this way nanowires show very strong emission compared to nanowires without shell layer. Illustrated growth process for growing radial heterostructures can be seen in Figure 2.3. The process starts exactly as same as axial nanowire growth and we grow first homogeneous nanowires as a core layer. This core layer is grown via vapor-liquid-solid and after a period of time for core layer growth, growth conditions are changed and system becomes completely different. New system conditions should make vapor-solid mechanism dominant for the rest of growth because growth temperature is changed and it favors

13

different growth mechanism. As long as we supply different source vapors and vapor-liquid-solid mechanism is not favored, we can get epitaxial growth on the nanowire surfaces. So far many groups have studied core/shell and core/multi-shell nanowire structures and highly efficient core/multi-shell nanowire based LEDs were demonstrated using MOCVD [39]. Even though some of these growths were performed in one step using the same experiment, some of them were grown in two steps. For two steps experiments, they grow first the core layer and completely cool down the furnace and then heat up the furnace again to the different temperature to grow the shell layers.
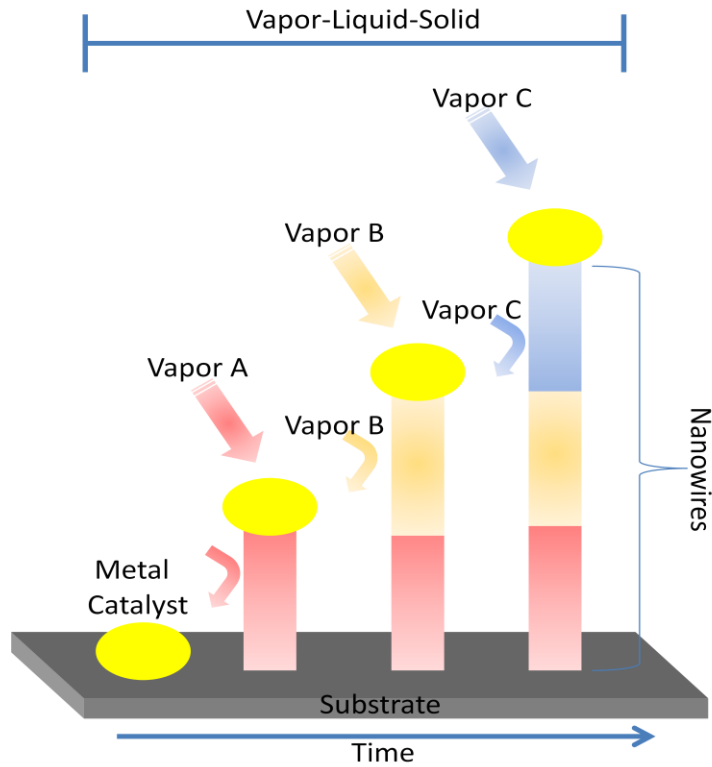
Figure 2.2 – Axial Nanowire Growth Sequence
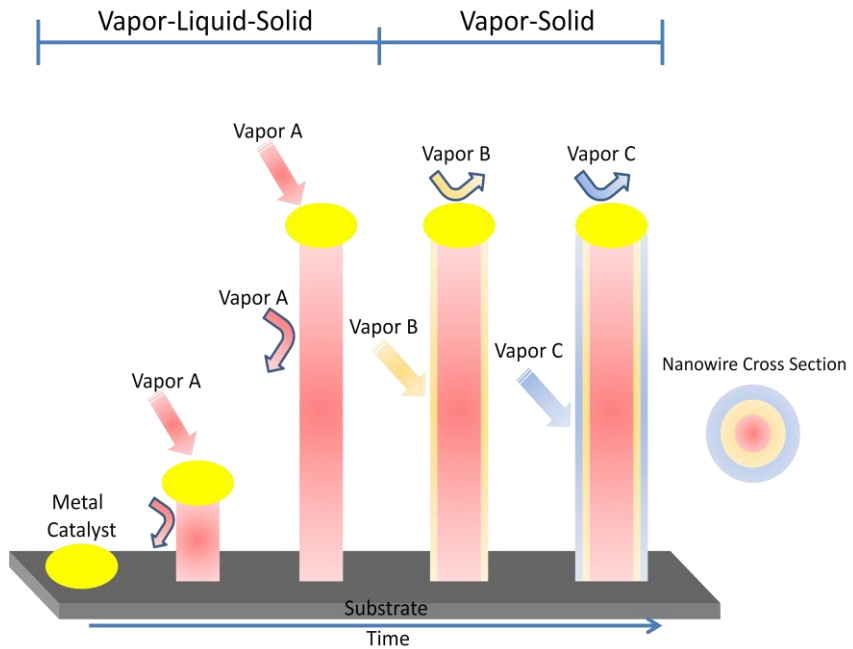
Figure 2.3 – Radial Nanowire Growth Sequence

15

2.3 The influence of Catalyst

Material of catalyst is critically important for nanowire growth because the diameter of nanowires and some other properties depend on the catalyst droplet and it can cause some problems in material which affects the way device works. First of all, gold migration can occur and this affects the nanowires` size and shape. Some nanowires are grown long but others cannot be. It is mainly owing to gold migration because gold has mobility and it always wants to go more intense region during the growth and this stops the growth on those nanowires. The reason is to cease growing that if there is no catalyst, nanowire cannot be continued growing. Having conic shape or some short nanowires compared to others are also the effects of this issue on the nanowires. All these effects can be seen in Figure 2.4. In order to eliminate this problem, catalyst droplets can be annealed prior to growth. If they are annealed at the temperature which catalyst has the highest mobility, the problems caused by immigration can be eliminated. Further information can be obtained from [38].
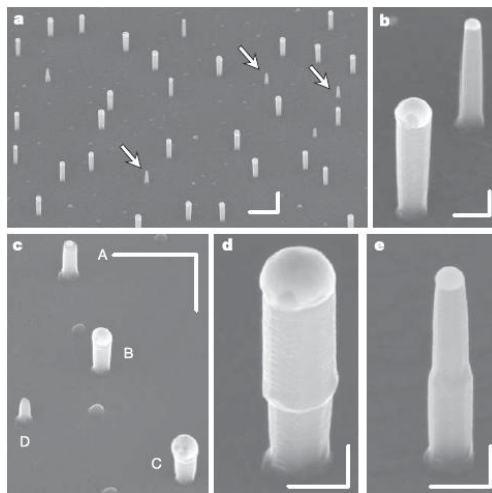
Figure 2.4 – The effect of gold migration

16

Second, gold is a deep level impurity for some material such as Si. If gold is used as a catalyst, it will create impurity states and thus electrons on these states want to recombine with holes and finally emission occurs from those states not from the band edge in case of Er-Si nanowires. So, this released energy cannot have enough energy to excite Er atoms. Therefore, this affects the emission intensity and it becomes weaker. A Korean group discussed this issue in detail and the best way to accomplish this problem is to use platinum as a catalyst because the impurity energy level of platinum is higher than the conduction band energy of Si. This process can be well understood on the figure 2.5 and further information can be found elsewhere [1]. Of course this is not only a problem for Er-Si nanowires, it can also be a problem for other nanowires. Due to these problems, some groups try to use new method that does not require metal catalyst to grow nanowires, and a team at Hokkaido University has used selective-area-metal-organic-vapor phase epitaxly to grow III-V nanowires and their heterojunction. Furthermore, type of material used as a catalyst is very important because the solubility rate of some precursors into the catalyst is very low and it affects the growth. For instance, the solubility of Indium into gold is very low and thus we have very less Indium material in InGaN nanowires grown via Au catalyst. Although this is not the main problem of this issue, it also has some influence on it. In order to eliminate this problem, different type of metal catalyst can be used.
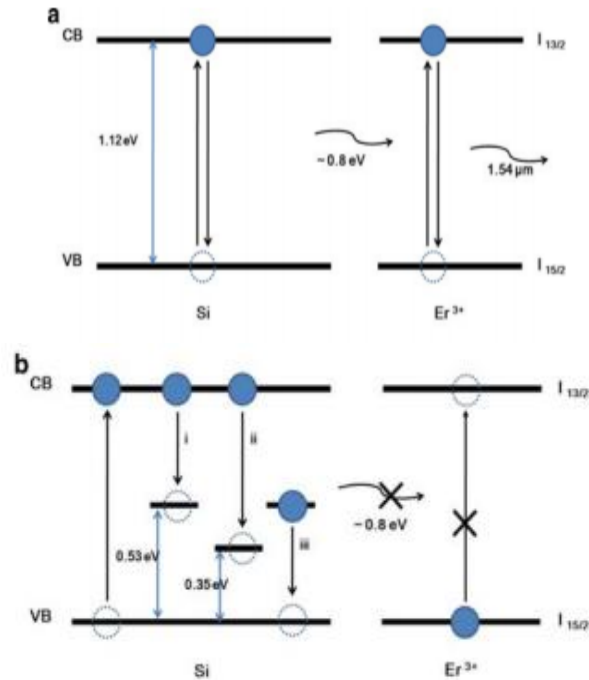
Figure 2.5 – Energy transfer mechanism (a) without deep level (b) with deep level impurity states.
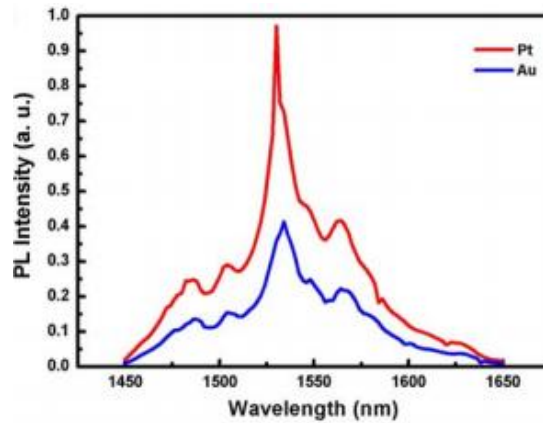
Figure 2.6 - The difference of the PL spectrum of the Er-Si nanowires grown with different catalyst material.

As we can understand from all of these aforementioned issues, catalyst plays a very critical role for growing high quality materials. Since we want to use nanowires for optical applications, those problems caused by catalyst should be carefully considered.

18

Chapter 3

SYTHESIS AND CHARACTERIZATION METHODS

3.1 Chemical Vapor Deposition (CVD) Growth System

In order to synthesis nanowires, there are many growth techniques which require different preferred growth conditions even for same kind of nanowire. Although there are many techniques to grow nanowires nowadays such as Laser ablation, Molecular Beam Epitaxy (MBE), Thermal Evaporation and Metal-Catalyzed Chemical Vapor Deposition (MOCVD), we will go into the detail of chemical vapor deposition (CVD) technique because nanowires in this thesis were synthesized via this technique.

CVD is a very widely used chemical system to grow high purity and high performance solid materials. Since the control of growth conditions is much easier with CVD system, many groups use the CVD to synthesis semiconductor nanowires or thin film. The idea behind it is simple and similar with thermal evaporation process. In CVD system, wafer is exposed to volatile source materials that react or decompose on the surface of the substrate. Usually, precursors are put into the middle of the furnace where the temperature is very high and substrates are put into the lower temperature zone. When the heat is applied to the furnace, source materials evaporate or sublimate and the carrier gas supplied from the outside carries vaporized source towards the substrate and finally, when they reach to the substrate, metal catalyst absorbs them and once the metal catalyst is supersaturated, nucleation event occurs and we start to grow nanowires between

solid and liquid interface. A basic CVD system used in this study to grow NWs will be explained and visualized in Chapter IV.

3.2 Optical Characterization Technique

3.2.1 Photoluminescence (PL) Spectroscopy

Photoluminescence spectroscopy is one of the most fundamental techniques to study the intrinsic and extrinsic optical and electronic properties of direct band-gap semiconductors. What makes it very significant is that it is contactless, sensitive and nondestructive technique and it also gives direct information about recombination and relaxation processes in materials. Basically, this technique contains a few processes which are optical excitation, absorption, relaxation and emission, respectively. First of all, under optical excitation whose energy is larger than band-gap of the material, material absorbs photons creating electron-hole pairs. Then, these e-h pairs relax to lowest energy level available, which is usually the band edge, by following recombination. As a result of recombination process, material emits other photons whose energy is less than absorbed photon. The energy of the emitting photon is determined by the band structure of semiconductor and this is usually equal to the band gap energy of the material. Meanwhile, it is important to note that the absorption spectrum of any material is always broadened than the PL spectrum. The reason for this is that absorption process occurs on all over the band as long as the photon energy is large enough, but emission occurs just on the band edge. Recombination process can be divided into two which are radiative and non-radiative recombination processes. A photon is emitted in radiative recombination process and in non-

radiative process, either a phonon or long wavelength photon with phonon is emitted. Phonon generation process is not a desirable process for any optoelectronic devices because this process creates heat and the luminescence efficiency of the device is reduced as heat increases in the device. Relation of the temperature with integrated luminescence intensity I (T) can be expressed with the following equation:

$$I(T) = \frac{I_0}{1 + \alpha e^{(-E_T/kT)}} \quad [40]$$

where E_T is activation energy, T is temperature and α is radiative rate parameter of the material. As can be seen from the equation, when the T increases, overall luminescence intensity is being decreased. Radiative recombination process is also divided into a few sub mechanisms. Those are band-to-band, conduction band-to-acceptor, donor-to-valance band, and donor-to-acceptor and exciton recombination, respectively. In terms of direct band-gap material, band-to-band recombination process is usually dominant and this is responsible for light emission. If some impurities are introduced in the material, donor-to-valence band, conduction band-to-acceptor and donor-to-acceptor recombination process also become possible. In addition to those, when electron-hole pairs are coupled by Coulomb interaction in material, excitons is formed and those can also recombine radiatively. If the thermal energy (kT) at the device operating temperature is less than exciton binding energy, excitonic recombination dominates the luminescence spectrum and makes the emission line narrow. For II-VI material, excitonic recombination process usually dominates due to the fact

that exciton binding energy of these materials is larger than any other materials such as IV and III-V. The luminescence energy from the material varies depending on the type of recombination process and those are listed in table 3.1.

Table 3.1 The luminescence energy of a material depending on the type of recombination process.

Recombination Process	Released Energy	Annotation
Band-to-Band	$$hv = E_G = E_C - E_V$$	E_G -Band Gap Energy E_C -Conduction Band Energy E_V -Valance Band Energy hv -Released Energy (E)
Conduction Band-to-Acceptor	$$hv = E_G - E_A$$	E_A -Acceptor Ionization Energy
Donor-to-Valance Band	$$hv = E_G - E_D$$	E_D -Donor Ionization Energy
Donor-to-Acceptor	$$hw_{DA} = E_G - E_D - E_A + \frac{e^2}{4\pi\varepsilon\varepsilon_o r_{DA}} - mhw_{LO}$$	$\frac{e^2}{4\pi\varepsilon\varepsilon_o r_{DA}}$ -Due to Coulomb interaction. Donor has + and acceptor has − effective charge. This causes Coulomb interaction. r_{DA} is distance between Donor and Acceptor in e-h pair. mhw_{LO} -Optical Phonon (LO) replica
Exciton	$$hv = E_G - E_X$$	E_X -Exciton Binding Energy

3.3 Structural Characterization Techniques

3.3.1 Scanning electron microscope (SEM)

SEM is a type of electron microscope and a very good characterization tool to image the surface of a sample by scanning it with a high energy electron beam. Basically, electron gun emits electrons and these electrons travel through the demagnification stages to scan a region on the specimen. When the electrons interact with the atoms of a sample, serious of signals containing many information are created. Those signals are secondary electrons (SE), backscattered electrons (BSE), X-rays (EDS), electron-beam-induced current (EBIC) and

cathodoluminescence (CL), respectively. (See Figure 3.1) These signals can then be used to modulate the monitor intensity and therefore build up a two-dimensional map of the near-surface topography, composition and possibly electronic nature. The SEM measurements in this work were performed using field-emission environmental scanning electron microscope (XL30 ESEM-FEG) from FEI company. XL30 ESEM-FEG uses Schottky field emission gun for outstanding observation performance of potentially problematic samples for conventional high vacuum SEMs. For this particular SEM machine, spatial resolution is 3 nm and accelerating voltage can be as high as 30 kV. Besides, the XL30 ESEM-FEG offers high resolution secondary electron imaging at pressures as high as 10 Torr and sample temperatures as high as 1,000°C. This means that wet, oily, dirty, out gassing, and non-conductive samples can be examined in their natural state without significant sample modification or preparation. For the taken SEM images in this thesis, 15 kV accelerating voltage and spot size 3 were used at secondary electron mode.
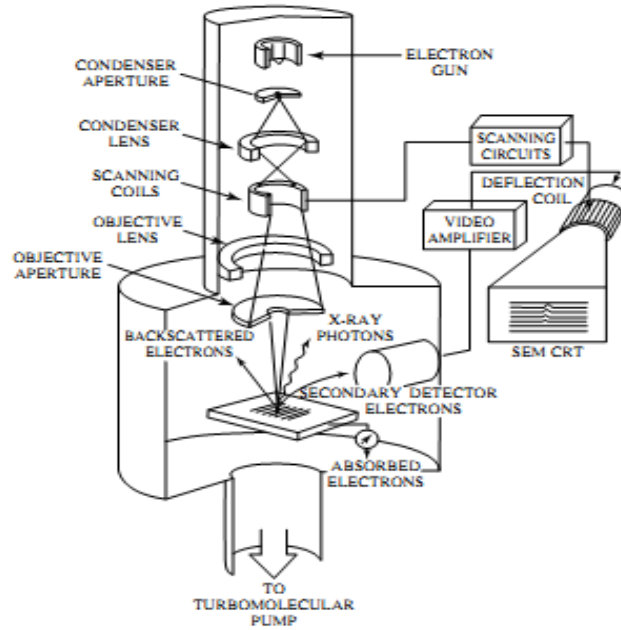
Figure 3.1 Schematic of a scanning electron microscope [31]

3.3.2 Energy-Dispersive Spectroscopy (EDS, EDX, or EDAX)

Most SEM system equipped with an energy-dispersive spectrometer (EDS) which detect elements and their composition in the sample. EDS can determine the energy spectrum of x-ray radiation which is emitted when primary electron interact with any atom. Although it is very useful technique, the accuracy is not as good as wavelength dispersive spectroscopy (WDS). The reason is that after primary electron interacts with an atom, it emits constant x-ray energy and this energy is used by the sensor. However, this particular sensor creates a number of e-h pairs depending on the following equation when $E_{x-ray} \gg E_G$:

$$\text{\#of e-h pairs} \sim= \frac{E_{x-ray}}{3E_G}$$

where E_{x-ray} is the emitting radiation energy from an atom and E_G is the bandgap of the material used in the detector. Depending on number of e-h pairs, current is created in the detector, and this flowing current determines the elements in the sample. If elements` radiation energies are close to each other, EDS cannot discriminate because in this case, number of created e-h pairs becomes almost same. Regardless this is overall a good and easy technique to have a general idea not precise about the elements and their composition in the sample. In this work, EDS analysis were performed using XL30 ESEM-FEG with 20kV acceleration voltage using spot size 5.

3.3.3 X-ray Diffraction Spectroscopy (XRD)

X-ray diffraction is a versatile and non-destructive technique which provides us information about chemical composition and crystallographic structure of materials and thin films. In a crystal, atoms are distributed in an order and they form a serious of parallel planes and those are separated from another plane by a distance'd'. The distance varies depending on the type of material and its nature. In a crystal, there are a number of oriented planes and each group of plane has its own d-spacing. The idea of XRD relies on the Bragg`s law and this is applied to all these planes. When X-ray beam with a wavelength lambda (λ) is shined onto a crystalline material, diffraction occurs only when the difference of distance traveled by rays, reflected from tandem planes, is n times of wavelength (λ) of incident beam. The principle behind it can be understood much better from Figure 3.2.
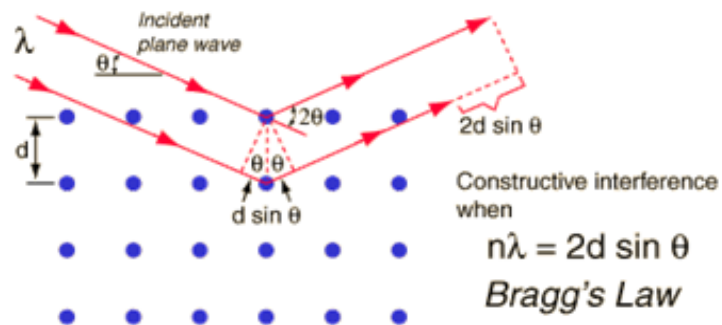
Figure 3.2 Principle of Bragg`s Law (taken from http://hyperphysics.phy-astr.gsu.edu/hbase/quantum/bragg.html)

By utilizing Bragg`s law, we can obtain a number of key information for the materials; for example, we can measure average spacing between layers, determine the orientation of single layer, find the crystal structure of unknown materials, and measure the internal stress of any crystalline region. It is also important to note that the shape and full width at half maximum (FWHM) of XRD peaks are very important and those give us information about particle or grain size and residual strain. For instance, if we see a broad peak on XRD pattern, we can think that there is some strain, and the crystalline quality is not as good as it should be.

X-ray diffraction patterns in this work were taken using the PANalytical X'Pert Pro Materials Research X-ray Diffractometer. This Diffractometer can analyze thin films, single crystals and powders from room temperature up to $900^{o}C$ using CuK_{α} radiations (λ= 1.54178 A).

Chapter 4

EXPERIMENT SETUPS

4.1 CVD Setup

In our CVD laboratory, we have three horizontal quartz tube furnaces. One of them is a Lindberg/Blue M split hinge three zone tube furnace which gives a chance to set all three zones to the different temperatures (up to 1200 C for short growth and 1100 for continuous growth) independently from the each others. Other two furnaces are single zone furnaces which can heat the reactor up to 1100 C. In this thesis, Lindberg Blue M three zone furnace was used to grow nanowires and belts. Therefore, we will give detail information for this particular furnace and the complete system.

Basically, we have a three zone furnace equipped with a 4` long and 1.5" wide horizontal quartz tube in where reaction occurs. Heating elements heat up the quartz tube from up and bottom side and hence the temperature inside the tube is almost uniform. This kind of CVD system is called hot wall CVD system. In addition to the hot wall CVD system, there is also a cold wall CVD system in which just substrate is heated. Since this kind of CVD setup is not available in our group`s laboratory, we used a hot wall CVD system for all kind of semiconductor nanowire growths.

There is inert gas supply into the reactor via ultra Torr Swagelok reducer (1.5" to 1/4"). The aim of this inert gas is to take the vaporized source to the substrate surface. It is important to note that amount of flow supplied into the reactor is very important and thereby some devices are required to keep the flow

rate in appropriate level. If the flow is too high, it acts like a blower and the reactions cannot be occurred on the substrate surface or growth rate will be very fast which make the quality of the product very bad. In order to control inert gas flow, MKS mass flow controller (MFC) is connected to the regulator of the cylinder and MKS read-out is also connected to the MFC. We just set the desired flow rate from the read out and it sends the necessary signals to the MFC to change the opening of the relay for supplying the desirable gas flow. Our MKS brand Read-Out has four channels and those can control four different MFC units individually. In our lab, we use just three channels and those are connected to the three different MFC unit to control the Nitrogen (N2), Ammonia (NH3), and Argon+5% Hydrogen (Ar+5%H$_2$) gas flow. N2 and Ar+5%H$_2$ are used as carrier gas, and NH3 is used as a source material for III-N semiconductor Nanowires growth.

To the right hand side of the tube, pump is connected to get away the volatile products and keep the pressure stable inside the reactor. On our system, ULVAC GLS series oil sealed rotary pump is used. Since the growth occurs in moderate pressure unlike MBE or MOCVD, rough pump is usually a good choice for CVD systems. We can evacuate our CVD system down to 5×10^{-4} Torr using ULVAC GLD series pump. In order to control the pressure and keep it stable, we have a few more equipments between pump and quartz tube. We have two manometers to measure pressure inside the reactor and there is a read-out connected to those manometers to read the pressure. One of these manometers is sensitive up to 1 Torr and the other one is sensitive up to 1000 Torr. By this way,

we can measure the pressure very accurately from 5×10^{-4} to 1000 Torr. Also, we have a variable valve to set the desired pressure inside the tube. In order to make the pressure stable, manometer read out and variable valve controller communicate and desired pressure can be obtained very precisely by utilizing these tools. The detailed picture of our system and all these tools can be seen in Figure 4.1.

Meantime, it is important to mention that controlling the temperature of the three zones separately gives us unique opportunities because for some alloy nanowire growths, different source materials require different temperatures and by using our furnace, we can easily set the desired temperatures to grow alloy nanowires. When we use the different temperature for different source materials, we put ceramic fiber isolation material on the boundary of the two zones and in this way we can keep the set temperature inside each zone.

(a)

(b)
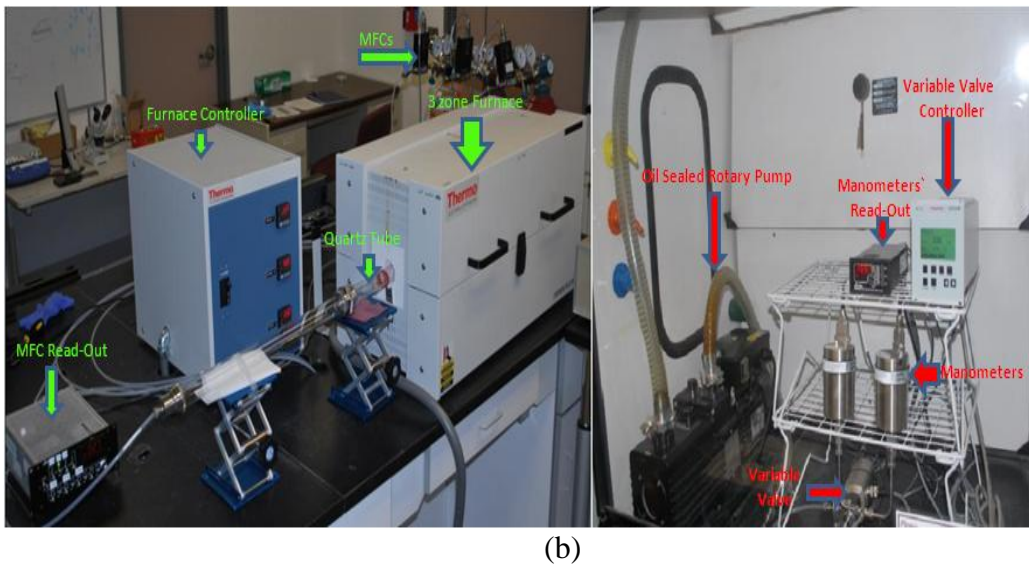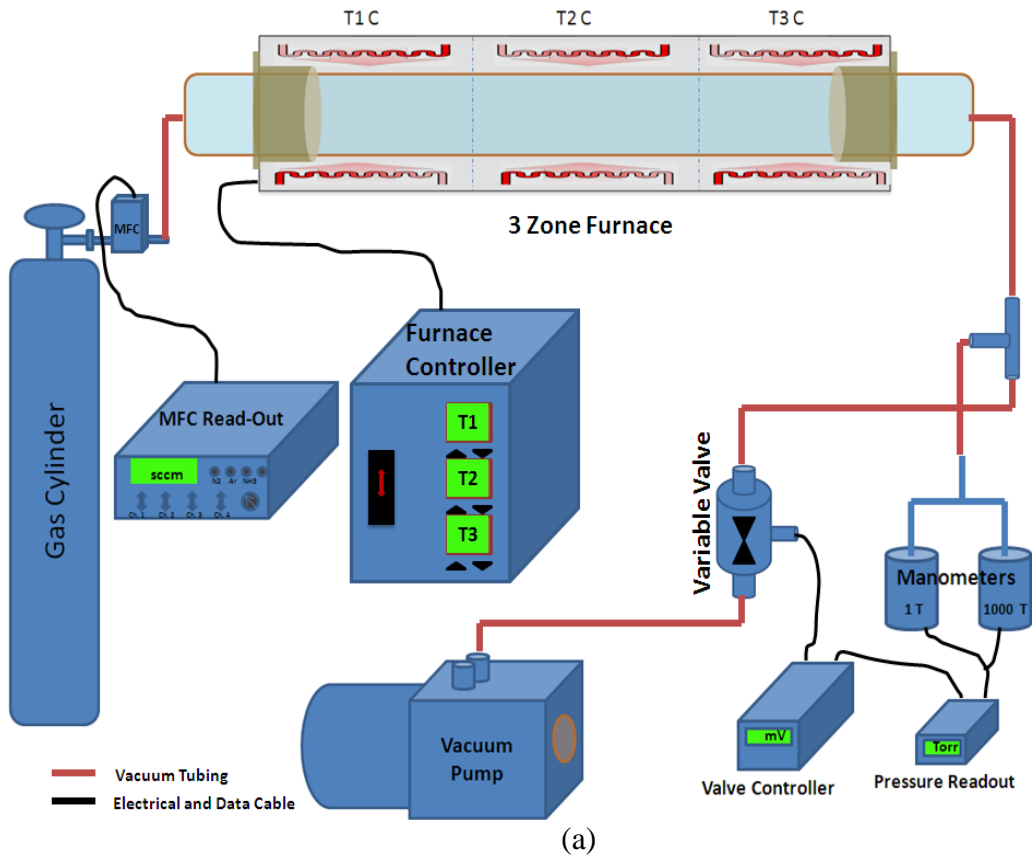
Figure 4.1 Schema of our Chemical Vapor Deposition system for growing Nanowires (a) and real picture of the system (b)

4.2 Micro-PL Setup

In our optical lab, we have four micro-PL setups designed for measuring different wavelength ranges from ultraviolet (UV) to Mid-Infrared (MID). These four setups are two UV/Visible, Near-Infrared (NIR) and Mid-Infrared (MID) micro-PL setups. A schematic of the one of the UV/Visible micro-PL setups is shown in Figure 4.2 and the other three setups have very similar construction. For the studies in this thesis, we just utilized UV/Visible and NIR Micro-PL setups.

Micro-PL setups basically have a few key components and those are as follows;

(1) Lasers

In our lab, there are two main laser systems and one small diode laser system. Two main lasers, which are used for comprehensive experiments, are Spectra-Physics mode-locked Ti:Sapphire pulsed laser system (Tsunami) and Quanta-Ray INDI pulsed Nd:YAG Laser. These two are equipped with a tripler system to provide second and third harmonic oscillation. Ti:Sapphire laser system delivers a range of wavelength from 690 nm to 1080 nm with a range of pulse width from 60 ps to 50 fs and also, 2nd. (~395 nm) and 3rd. (~266 nm) harmonic wavelength sources can be obtained utilizing the tripler system. On the other hand Nd:YAG is a Q-switched, nanosecond, frequency quadrupled laser and has built in second, third and fourth harmonic generators to deliver ns laser pulse at 1064nm, 532nm, 355nm, and 266nm, respectively. Another small laser, which is used for quick optical experiments, is PDL 800-B PicoQuant picosecond pulsed diode laser and it can deliver 405 nm laser pulses.

31

(2) Delivery System

In order to deliver laser beam to excite the sample and collect the PL signal from the sample on a spectrometer, many optics such as mirrors, lenses and beam splitters, should be used. However, those are has different reflection, absorption and transmission efficiencies and each individual optic acts different for distinct wavelengths, hence optics should be chosen accordingly. We chose, for instance, aluminum coated mirrors for UV/Visible setups and silver coated mirrors ($\lambda > 450nm$) for NIR setup because these coating materials have the most appropriate values in the corresponding wavelength regions. Meanwhile protected gold mirrors ($\lambda > 650nm$) are used for especially MIR systems because the reflectivity has the highest value near MIR range.

(3) Spectrometers

Emitted PL signal from a sample is collected via objective lens then this collected signal is collimated and focused into a small slit on the spectrometer to be analyzed. In our optical lab, there are three different spectrometers. Those two are the TRIAX series and the other one is the iHR series spectrometers from JOBIN YVON INC. All these spectrometers have an optional triple grating turret to give us flexibility in the choice of the gratings for optimum resolution and desired spectral range. The three selectable gratings are 600 g/mm, 150 g/mm, and 300 g/mm for MIR and NIR setups, 2400 g/mm, 1200 g/mm, 300 g/mm for UV/visible (TRIAX) setup and 1800 g/mm, 1200 g/mm, 600 g/mm for another UV/visible (iHR) setup, respectively.

(4) Detectors

It is necessary to use different kinds of detectors to cover the distinct wavelength regions due to the fact that different core materials used to build detectors has different band gap energy and the energy lower than the detectors bandgap energy cannot be detected. Therefore we have to use different types of detectors to cover the different spectral regions. In our lab, two liquid nitrogen cooled CCD detectors are equipped for UV/Visible setups to cover the wavelength range up to 1.1 μm. On the other hand liquid nitrogen cooled InGaAs detector is used for MIR setup to cover region from 1μm to 5μm and liquid nitrogen cooled InSb detector is equipped for NIR system for the 700 nm to 1800 nm spectral region. In this work, only CCD and InGaAs detectors were used.

(5) Imaging Systems

In order to see the small sizes on the sample, high magnification lens is necessary to be used, and light source goes through this objective lens to illuminate the sample and then reflected light sources are collected by the same objective and reflected to the camera and/or eye pieces of the microscope. After all of these processes, the information is sent to the computer to show the picture of the sample simultaneously. For our UV/Visible (TRIMAX) setup, there are both eye piece and camera options because the system is integrated with a dark field optical microscope.

(a)

(b)
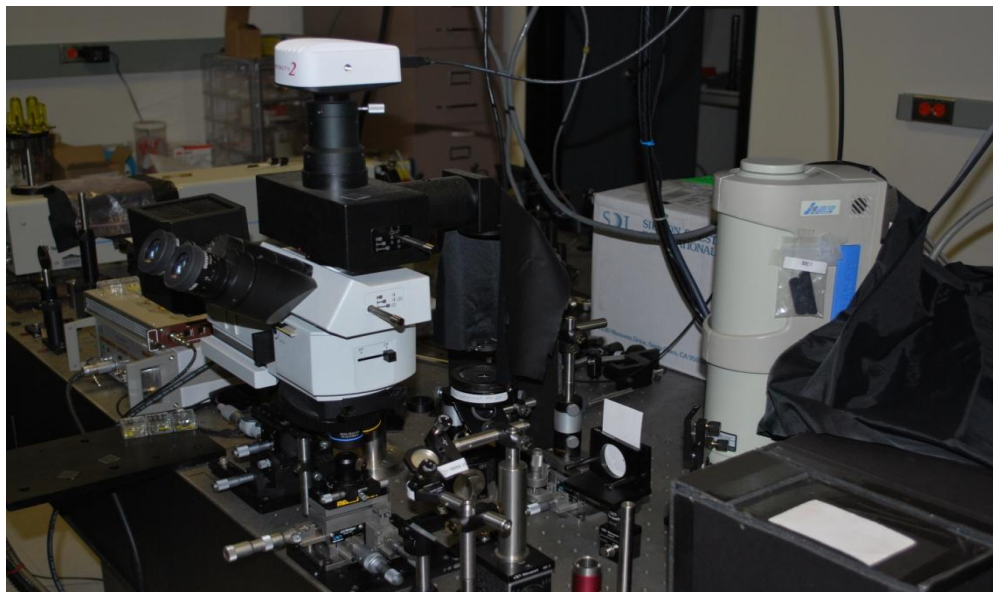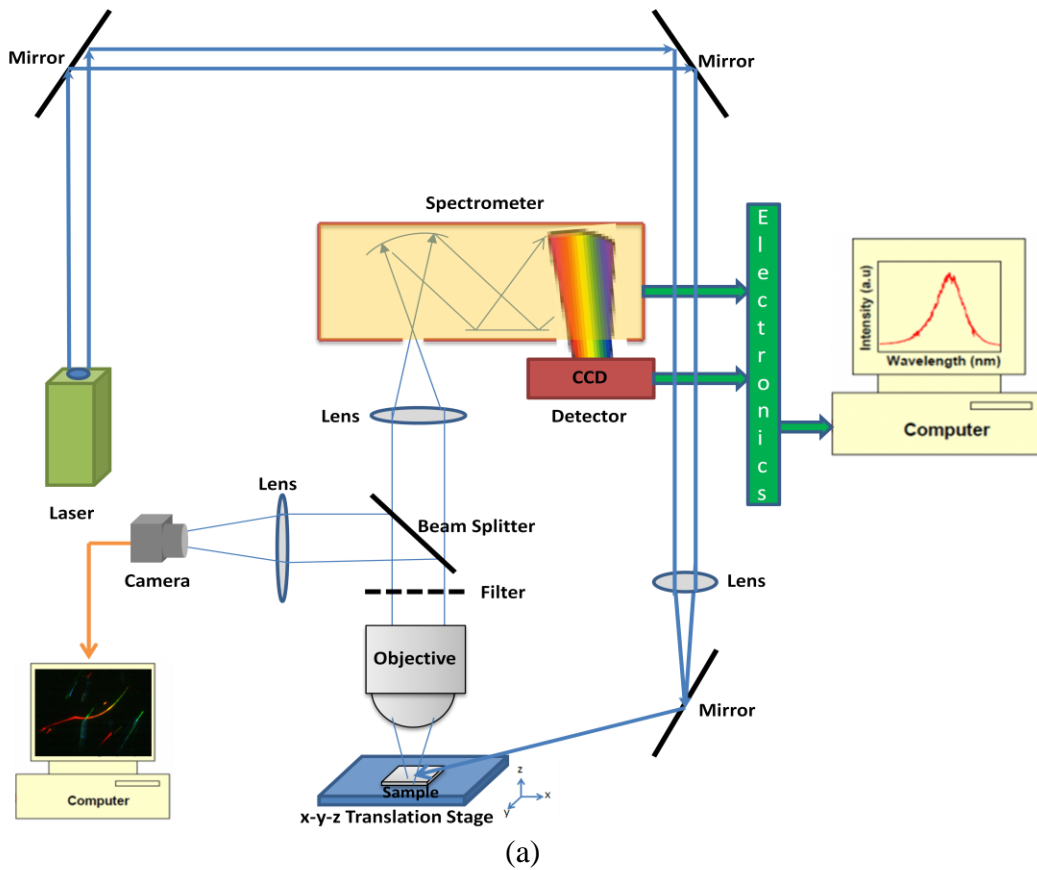
Figure 4.2 Schematic of UV/Visible Micro-PL setup (a) real picture of the setup (b).

Chapter 5

ERBIUM CHLORIDE SILICATE (ECS) NANOWIRES

5.1 Introduction to Silicon Photonics and Erbium doped Silicon Compounds

Silicon photonic is one of the most attractive research area in today`s developing technology. The compatibility with the ripe silicon integrated circuit (IC) technology makes it very attractive. Silicon wafers are cheaper than any other semiconductor materials and it is possible to make microprocessors with millions of components just on a penny size chip. Since there is plenty of silicon source in nature, ICs are offered at very low price and this makes them widely used in consumer electronics. For a decade, researchers have been extensively working on creating low-cost silicon photonics for real devices by exploiting well developed IC industry and it is believed that silicon photonics will change the way of current technology very dramatically in a good way.

Silicon has excellent properties and those are still effective and even stronger in photonic devices. Those are, for example, high thermal conductivity-~10x higher than GaAs, high optical damage threshold which is also 10x higher than GaAs and high third-order optical nonlinearities [3]. As shown in absorption spectrum of silicon (Figure 5.1), silicon has a window between 1.1μm and nearly 7μm and this window offers very low loss which is the most desirable property for some applications such as fiber optic communication.
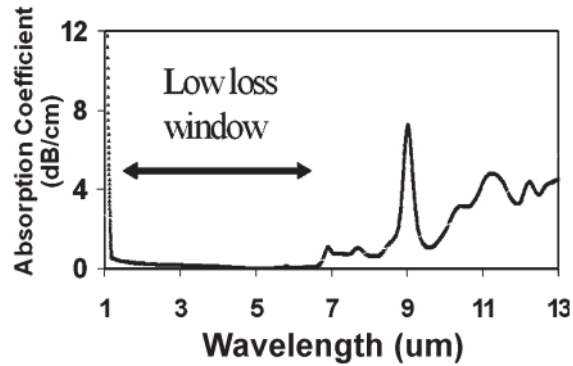
Figure 5.1 Absorption spectrum of Silicon [3]

Due to low cost substrates and mature enough fabrication techniques, silicon photonics is very important path way for mass production of the new optical components and devices which can combine electronics and photonics technology. So far, many silicon photonic devices have been realized and one of the most important ones is the optical interconnects which are very fascinating. Optical interconnects can basically eliminate the signal delay of the electrical connection as happen on the copper interconnects and as well as those reduce the power consumption of the system. In order to build more sophisticated lab-on-chip devices, Si based components are necessary to be realized. Those important components are basically silicon based   light modulators, detectors, optical waveguides, interconnectors and light emitting diodes (LED). So far these components have been successfully built but efficient silicon based LED remains in abeyance because silicon is an indirect band-gap material and it hardly emits light. If highly efficient silicon bases LEDs are fabricated, this will change the current technology very deeply and new Si based compact devices on the same chip can be realized.

36

As a matter of fact Silicon Nanocrystal and highly porous Silicon can emit red, green and blue lights and the efficiency of the LEDs can reach up to 1% which is almost 10000 times better than bulk silicon; however, this is not enough for commercial devices. There is more way to go before Nanocrystal and Porous Silicon LEDs become commercially available. In spite of the fact that 1% efficiency can be sufficient for some integrated light-emitting displays, the speed of the device cannot be very fast and the switching speed can cause some problems. Since silicon is not a direct band-gap material, light emission occurs if an additional process involve to the transition process. As a result of this additional process, light production occurs in longer time than direct band-gap materials which means that more heat is created in the system and this dramatically limits the light output. Due to this additional process, silicon LEDs cannot be switched very fast like 100 megahertz or 1 gigahertz rates needed for optical fiber communication. That is the main problem for Silicon based LEDs and many approaches are considered to achieve these aforementioned limits. Those approaches are, for example, using impurity level for light emission, and using rare earth materials in Silicon which is the most important one.

The realization of efficient light emission and amplification in erbium doped optical fibers has attracted the attentions on Erbium doping in Silicon. However, silicon is not a good host material for erbium and this leads to have weak light emission from the structure that is not desirable for many applications. This problem is believed due to back transfer of the energy from exited Erbium

ions to silicon via trap states and having low Erbium concentration in Silicon which is the most important one.

Light emission and amplification around 1.53μm is very significant wavelength region for optical fiber communication and can be very important for the future Nanophotonics systems. As we showed in figure 5.1, silicon has low absorption around that region and especially 1.53 μm emission line is very close to 1.55μm wavelength which offers the lowest propagation loss for optical fibers. Since the emission line of erbium ions at 1.53μm is quite strong, Er-doped or compound materials are widely used in communication systems and can be used for many unique applications. However, in order to produce sufficient optical gain, Erbium concentration in Silicon should be very high; otherwise we cannot achieve the fabrication of lab-on photonic devices on a penny size chip which is our main interest.

People can usually achieve Erbium concentration in Erbium doped Si or SiO_2 below $10^{20} cm^{-3}$ [7] which is not enough for providing high optical gain. Even if it is enough, the method to get this amount of concentration involves multiple steps not compatible with silicon fabrication techniques. People usually incorporate Erbium in crystal silicon using different methods such as magnetron sputtering and solid phase epitaxy, and then material has to be annealed at higher temperatures to re-crystallize. High temperature is not good for silicon based device fabrication owing to the fact that conventional growth temperature for Silicon based devices is around $550 - 600^{o}C$.

38

In this study, we report the synthesis of new Erbium compound Erbium Chloride Silicate $(Er_3Cl(SiO_4)_2, ECS)$ single crystal nanowires. The Erbium concentration in our new material is at $1.6x10^{22}cm^{-3}$ which is 2-3 orders of magnitude higher than other Erbium doped materials. To our knowledge, this is the highest Erbium concentration up to date. Not only the Er concentration and photon life times are high for our new material but also light emission line at 1.53μm is much narrower than other Er-doped and Er compound materials. These features are very significant improvements to make the Silicon based compact devices on the same chip available.

5.2 Erbium Related Emission

Before explaining the synthesis of the ECS nanowires, it is better to have some idea about how the 1.53 μm emission occurs in ECS or any Erbium-doped/compound material. It is known that optical transitions in rare earth (RE) materials such as Erbium, Ytterbium and Neodymium, and many others, involve between the internal energy levels and these transitions are in charge for emitting photons. The emission is quite independent from the host material. When we grow some RE compounds or dope RE element in a host material, they always have a strong inclination of being in a 3+ electronic state that is called trivalent. The transitions from the Er^{3+} and many other RE^{3+} occur between 4f states. It is very important to note that these transitions are not possible in case of free ions; however, we can make it possible with a crystal field if we introduce RE^{3+} ions in to a solid. The crystal field splits each single state of free Er^{3+} ions into a

number of sub states whose energy is slightly different from others. This phenomenon can be seen in figure 5.2.
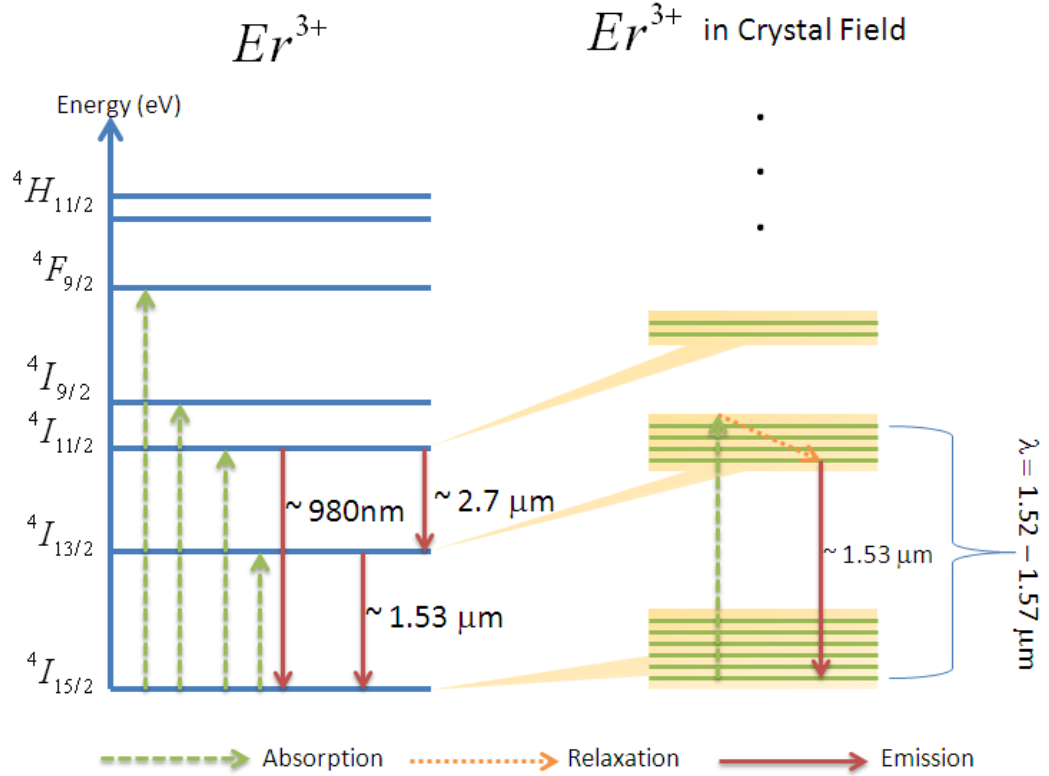
Figure 5.2 Energy Level diagrams of free Er^{3+} ions and Er^{3+} ions in a crystal field.

Incorporated Er^{3+} ions in a semiconductor material have an incomplete 4f electronic state ($[1s^2 2s^2 2p^6 3s^2 3p^6 3d^{10} 4s^2 4p^6 4d^{10} 4f^{11} 5s^2 5p^6 6s^2]$, $[Xe] 4f^{11}$) and this allows the intra 4f transitions when the structure is excited by an optical source whose energy is higher than the energy of related states. For ECS nanowires, we are interested in $^4I_{13/2} \rightarrow {}^4I_{15/2}$ transition where $^4I_{15/2}$ is the first excited state and $^4I_{15/2}$ is the ground state of the Er ions. Since $^4I_{13/2}$ is the first excited state with the energy of 0.8eV, transition between these states gives ~1.53µm emission which is the perfect wavelength region for fiber optic

40

communication. Although the strongest peak occurs at $1.53\mu m$, there are some weak peaks near 1.53 μm. The reason for having those small peaks is the splitting of main states into many sub states by crystal field in the solid.

As we said in this paragraph, emission is independent from the host material and occurs as explained; therefore obtaining high Er concentration in a solid is highly crucial.

5.3 ECS Nanowire synthesis

All of ECS nanowires in this study were synthesized using three zone open hinge CVD system as showed in Chapter 4, and the growths were performed by vapor-liquid-solid mechanism under catalytic conditions. As a catalyst, we used Gold (Au) and for different experiments, different thickness of gold layer was deposited using Denton Vacuum Desk II sputter coater. ECS nanowires were synthesized on both Si/SiO2 and quartz substrates. The reason to use different substrate materials is to see the effects of substrates on the growth kinetic. Prior to gold deposition on substrates, we cleaned the Si/SiO_2 or quartz substrates` surface using following recipe;

1- Place substrate into baker which has Acetone in it and put the baker into the ultrasonic bath for 3 - 4 minutes.

2- Move the substrate into another baker that has Isopropenyl alcohol (IPA) in it and put it into the ultrasonic bath as well for another 3 - 4 minutes.

3- Rinse wafers under deionized water for a while.

4- Dry substrate with Nitrogen.

Usage of these chemicals for cleaning the substrate surface has different tasks. Basically, Acetone dissolve Organic Residue on the substrate, IPA dissolves Acetone residue and distilled water is believed to dissolve IPA residue and other residue that cannot be dissolved by either Acetone or IPA. As a final step, nitrogen is blown to have a dry wafer surface. After all of these processes, wafers are ready to be sputtered and we generally use the sputtering time to indicate the thickness of gold layer on the wafer. For our particular sputtering machine, 120 sec. is ideal to have about 10 nm Au layer and in order to learn roughly the thickness of the gold layer using sputtering time; we make a simple calculation based on this comparison. Since we use sputter coater machine to deposit gold, a layer of gold not gold droplets is formed on the substrate; however, upon annealing, the layer breaks apart into small Au droplets which initiate the nanowire growth. The size and concentration of these droplets depend on the annealing temperature and layer thickness, respectively. Although this method is very simple, it is difficult to get uniform nanoparticles size and distribution.

Here, we will give a general picture of the ECS growth owing to the fact that we run plenty of experiments by using different configurations such as various thicknesses of gold layers, different source and substrate temperatures, different pressure and flow rates. Some of these experiments will be given in a table to make a comparison. For ECS nanowire synthesis, we used Aldrich Silicon powder -60 mesh, 99.999% as a Silicon source and Alfa Aesar Erbium Chloride (ErCl$_3$) micro beads 99.9% (metal basis) as an Erbium source. Some amount of source materials are put into quartz boats to introduce into the quartz tube. Prior

to introducing source boats, we cleaned the quartz tube using ethanol and after cleaning process, these quartz boats are put into the furnace. The location of the Si source was always kept at the middle of the 2nd zone which is also the center of the three-zone furnace because we need the highest temperature for the Silicon source and center of the furnace has the highest temperature value according to our temperature profile measurement. Then $ErCl_3$ within another boat is placed to the downstream of the furnace where the temperature is slightly lower than Si source temperature. After placing two boats, Si (100)/SiO2 substrates with gold deposition on it are put into the quartz holder which has five trenches to hold the substrates vertically. We usually put three or two substrates in the holder to make a comparison between substrates which have different growth temperature. After placing sources, the holder with substrates is put to the downstream of the $ErCl_3$ source boat. The distance between $ErCl_3$ and substrate holder varies for different experiments but for most of our experiments, we used it next to the $ErCl_3$ source boat. After placing all necessary sources and substrates, the quartz tube in three-zone furnace was evacuated to   100 mTorr using oil sealed rotary pump. In order to check the leakage in our system, we used a recipe as following;

     1-) Close the pump valve when it reaches to 100 mTorr

     2-) Let the system for 10sec without pumping

     3-) Check the new pressure value

     4-) If the ratio of pressure difference (new pressure value – 100 mTorr) to the time (10 sec) is less than 10, leakage rate of the system is fine. If it is more than 10, the system should be checked again.

After checking the leak rate, a constant flow of 62 standard cubic centimeters (sccm) $Ar + 5\% H_2$ is introduced into the system as a carrier gas through the mass flow controller and pumped along the quartz tube as shown in figure 4.1. The pressure of the system was kept between 2.2 and 3 Torr depending on the carrier gas flow. For ECS experiments, variable valve is set to 0 mV which makes the valve full open and thus we used the full capacity of the pump to get the pressure around 2.x Torr with gas flow during the experiment. The three zones were heated from room temperature to 1100 C - 1200 C, depending on the experiment, at the same time. All three zones were set to the same temperature values. So, since silicon in quartz boat was placed to the center of the furnace, source temperature of silicon became almost same with the set temperature. As we indicated before, $ErCl_3$ source and substrate holder were positioned downstream where the temperature is less than the set temperature of the 3rd zone. After the system is heated up with a rate of 60 C/min and kept at the set temperatures for some time, usually 90 min, , the furnace was allowed to cool down to room temperature with a rate of 7 C/min. The general picture of the locations of the sources and substrates for growing ECS nanowires are shown in figure 5.3 and also, the temperature profile inside the quartz tube is shown in figure 5.4 for better understandings of the experiments.
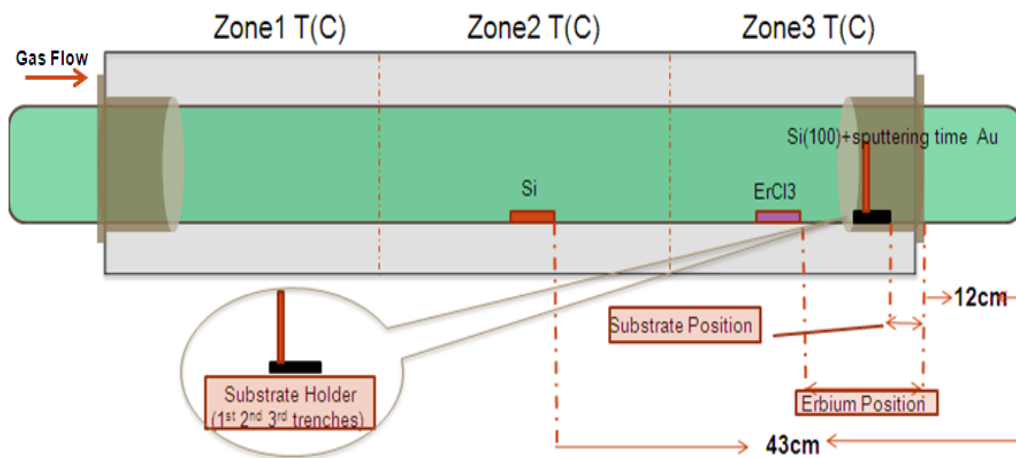
Figure 5.3 Basic scheme for ECS NW growth. Figure shows the location of the source materials and substrates in the quartz tube.
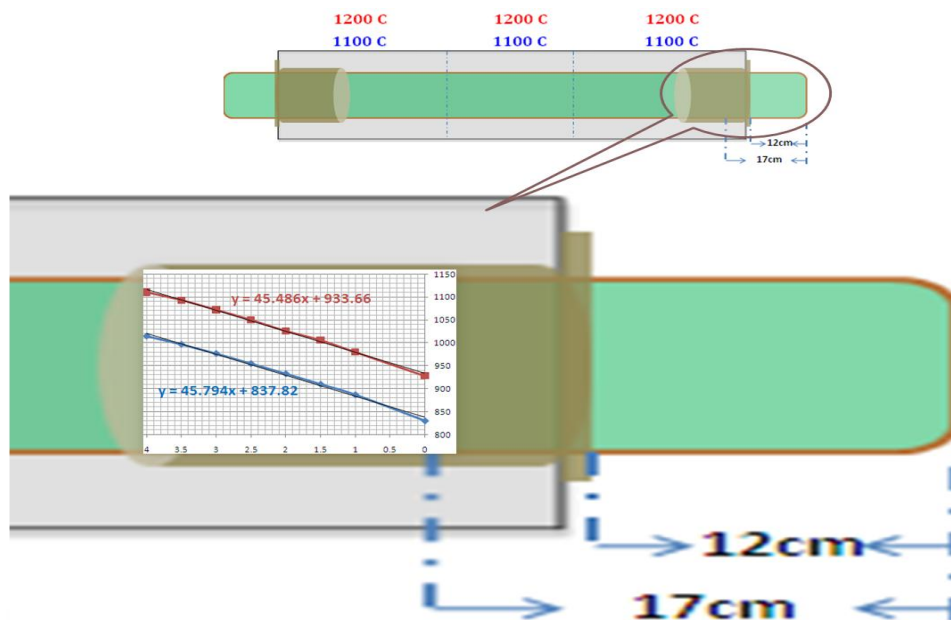
Figure 5.4 Measured temperature profile inside the quartz tube for ECS nanowire growths.

45

5.4 Characterization Methods

The surface morphology of the nanowires was examined by a scanning electron microscopy (SEM), and SEM images were taken using a Philips XL-30 field emission SEM machine equipped with an energy dispersive X-ray detector, operated at 15 kV. Also, energy dispersive X-ray spectroscopy (EDS or EDAX) analysis was performed using the same machine, operated at 20 kV, to find out the composition of our samples. Another characterization technique, X-ray diffraction spectroscopy, was also performed to find out the composition of our samples and figure out the atomic structure of materials and the crystalline quality of the sample using PANalytical X'Pert Pro Materials Research X-ray Diffractometer, which is equipped with a CuK_a radiation (= 1.54178 A), on the powder diffraction mode. Photoluminescence (PL) measurements were conducted using our near infrared (NIR) PL setup which has the similar construction with the UV/Visible setup. (See Fig. 4.2) For NIR setup, A Ti: Sapphire laser at 790 nm was used and beam was focused to the sample for optical excitation. The PL signal from the sample was collected and focused via optics to the entrance slit of a 0.10 m monochromator and detected by a liquid nitrogen cooled InGaAs array detector.

5.5 Result and Discussion

SEM images of some as grown samples on Si (100) with pre-deposited gold layer are shown in figure 5.6. The growth conditions for each sample are different and summarized in table 5.1. As seen in the images, there are distinct morphologies in the samples depending on the growth conditions; however, the

common think is that all the wires are grown in random direction; there is no a specific orientation for ECS nanowires grown on Si (100)/SiO2 substrate. In general, wires have diameter from several tens of nanometer up to one micrometer depending on the catalyst size and the length varies from several to more than twenty micrometer depending on the growth time.

In order to determine the composition elements of nanowires, EDS was performed and it shows the wires are composed of elements Si, Er, Cl and O. (see figure 5.5) Although SEM and EDS give us general information about the wires` morphology and the composition elements, those are not enough in some cases and we should have further information such as crystalline structure and quality to be able to evaluate the samples. Therefore, besides SEM and EDS, X-ray diffraction (XRD) was also performed on the ECS nanowires. For determining the differences between experiments, grown using distinct conditions, many XRD analyses were performed through this work, but two of them, here, will be discussed considering the growth conditions, their final structures and integrated PL emissions.

Element	Wt %	At %
O K	17.84	51.62
SiK	16.70	27.53
ClK	02.91	03.80
ErL	56.16	15.55
AuL	06.39	01.50
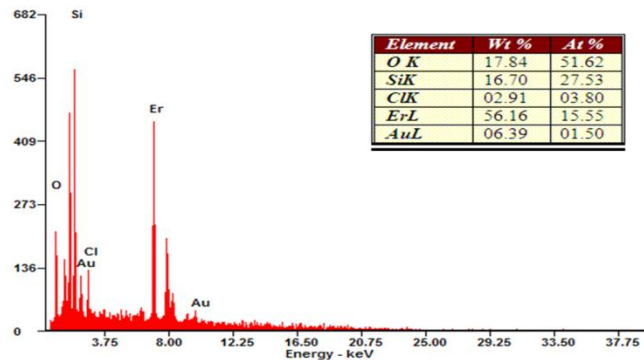
Figure 5.5 EDS spectrum of an ECS sample.

47

Table 5.1 Growth conditions of the experiments. (See figure 5.3 for the better understanding of the parameters.)

Sample	Pressure	Sbstr. Pstn.	ErCl3 Position	1st. Zone	2nd. Zone	3rd. Zone	Substrate Temp.	Au sputtering	Carrier Gas	Gas Flow	Growth Time
(a)ST-1-21	2.1 Torr	5cm	Next to Sbstrt	1200	1200	1200	935	500sec	Ar+5%H2	47/35sccm	98min.
(b)ST-1-24	3.5 Torr	6.5cm	Next to Sbstrt	1100	1100	1100	900	500sec.	Ar+5%H2	62/50 sccm	90min.
(c)ST-1-2	4.4 Torr	7cm	Next to Sbstrt	1100	1100	1100	930	100sec.	Ar+5%H2	62/50sccm	30min.
(d)ST-1-26	2.1 Torr	6cm	Next to Sbstrt	700/1100	700/1100	700/1100	890	500sec.	Ar+5%H2	62/5sccm	90min.
(e)ST-1-40	2,5 Torr	6cm	1cm	1100	1100	1100	890	500sec.	Ar+5%H2	62/50sccm	2hrs.
(f)ST-1-77	2.5 Torr	6cm	NExt to Sbstrt.	1100	1100	1100	890	700sec.	Ar+5%H2	70/58sccm	60min.
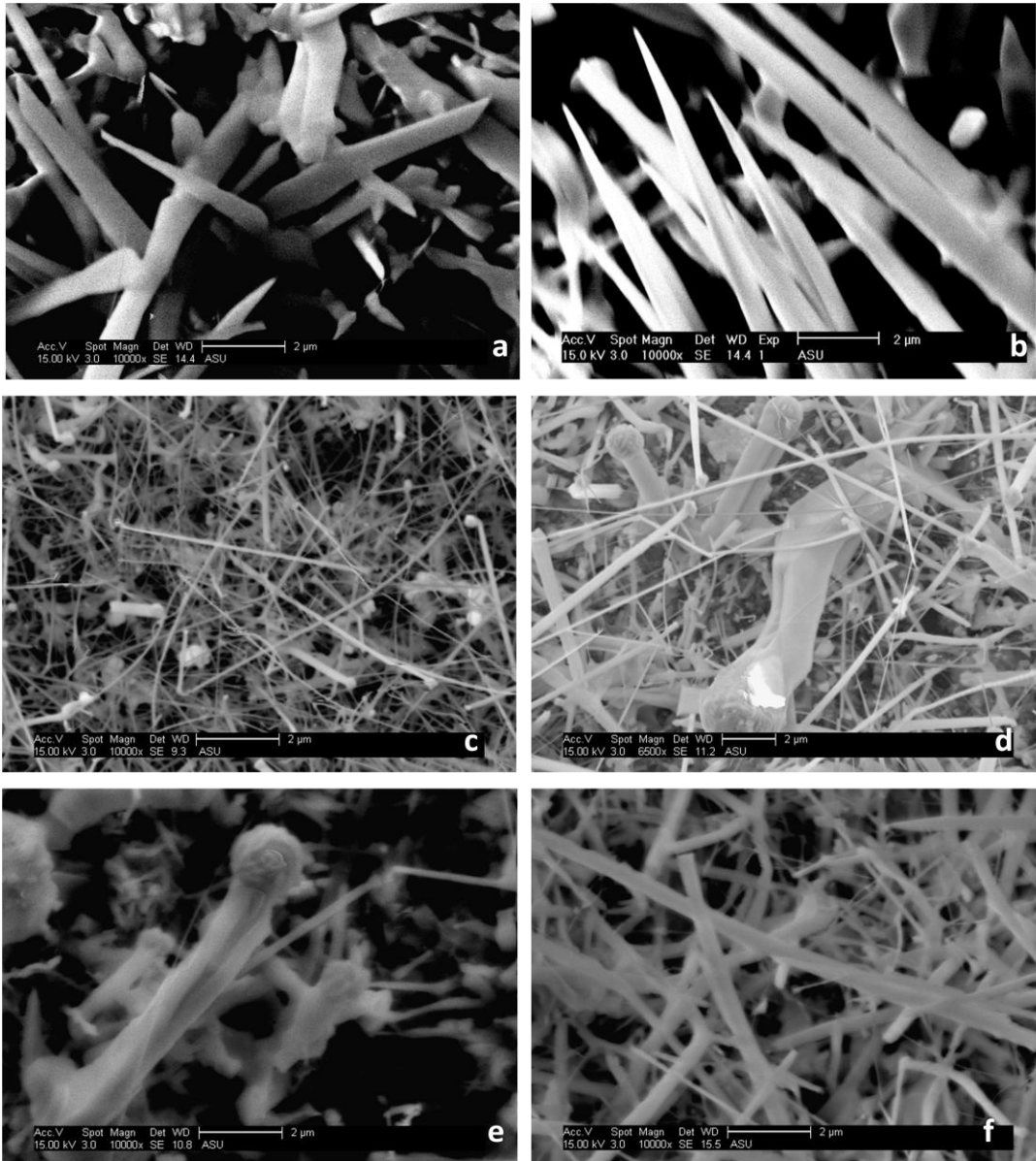
Figure 5.6 SEM images of the samples ST-1-21, 1-24, 1-2, 1-26, 1-40 and 1-77 from a to f, respectively.

48

Before going into the XRD analyses, it is better to mention the possible growth mechanisms which play a role in the formation of ECS nanowires. We believe that two main mechanisms involved into our experiments and the first mechanism is for growing ECS core/shell structures and the other one is for pure ECS nanowires. As a matter of fact, the first step for both mechanisms is same, but the second step can be different mainly depending on the growth temperature.

First of all, when the furnace is heated up, Si powder and $ErCl_3$ micro beads start to give some source in vapor form, however, since the Si source is always put to the highest temperature zone, the Si vapor is more active than the $ErCl_3$. Although we set all the three zone to the same temperature, $ErCl_3$ source boat is generally located inside the quartz tube holder which isolate some heat from the 3rd zone.(See figure 4.2)When the vapors meet with the substrate which has catalyst on it, nanowire formation is begun after the supersaturation. However, since the silicon is more active than the $ErCl_3$, silicon core is started to be formed first. After the formation of Silicon core, $ErCl_3$ is adsorbed and Si, $ErCl_3$, and O get into a reaction on the Si surface. As a result of this process, ECS shell layer is formed on the surface of the Si core. However, when we apply very high temperature to the 3rd zone of the furnace where we put $ErCl_3$ and Substrate next to each other, the chemical potential of the $ErCl_3$ is increased and the $ErCl_3$ vapor becomes more active and can compete with Si core or they start to incorporate into the catalyst at the same time. For the second growth mechanism, the process is started as same as the first one but due to higher energy under higher temperature, $ErCl_3$ vapor start to compete with Si core and the reaction

occurs on the surface of Si core. However, since ErCl$_3$ is more active in this case, Er, Cl, and O also incorporate into the Si core or they directly incorporate into the metal particles at the same time before letting Si core to be formed and finally we grow pure ECS nanowires without any Si core. When we compare the two different experiments relied on two distinct mechanisms, there is no much difference between them in diameter wise, but since for the second type of growth, the growth temperature is much higher, possibility of getting wider nanowires increases. So this makes our nanowires contain more Erbium ions compared to the others. Even if the diameters of two structures are same, pure ECS wires always contain more Er ions. If we recall that having high Er concentration is very crucial for sufficient optical gain, the second growth mechanism becomes very important for growing very efficient light sources operated at 1.53um. According to experiments done for this work, the key of having more efficient and much better nanowires in terms of crystal and optical quality is the growth temperature. The differences between samples grown using different growth temperatures will be shown utilizing XRD spectrums.

As indicated above, growth temperature plays a very crucial role for having pure ECS nanowires with good crystalline quality and this will be showed by comparing two experiments named ST-1-1 and ST-1-62. The growth conditions for these experiments are listed in table 5.2. The main differences between these samples are the growth temperature, Au sputtering time and growth time, respectively. All the other parameters are same as shown in table 5.2. As we indicated before, thicker gold layer always make the products wider and wires

50

become longer with longer growth time. According to SEM analyses of the sample ST-1-1 and ST-1-62, nanowires on ST-1-62 are much wider than ST-1-1 but on the other hand length of the wires is shorter for sample ST-1-62. Those results are consistent with what we said before. Since the Au layer sputtering time is 500 sec for ST-1-62, much bigger droplets can be formed and the nanowires are grown via those metal droplets. Also, since the growth time was 90 min for ST-1-1 which is 30 min longer than ST-1-62, we got longer nanowires compared to the others. The effects of these two notions are very clear and well accepted with the results of these two experiments and many other experiments which are not shown here. As can be understood, Au layer thickness and growth time change only the morphology of the products. Although the morphology is also very important for device applications such as nanowire lasers, crystal structure is more important for many device applications because the light emission becomes very efficient with a good crystalline material.

Table 5.2 Growth conditions for samples ST-1-1 and ST-1-62. For the position of source materials and the temperature profile inside the tube, refer the figure 4.1.

Sample	Pressure	Sbstr. Pstn.	ErCl3 Position	1st. Zone	2nd. Zone	3rd. Zone	Substrate Temp.	Au sputtering	Carrier Gas	Gas Flow	Growth Time
ST-1-1	2.5 Torr	7.5 cm	Next to Sbstr.	1100	1100	1100	955	100sec.	Ar+5%H2	62/50 sccm	90min.
ST-1-62	2.5 Torr	7.5 cm	Next to Sbstr.	1200	1200	1200	1070	500sec.	Ar+5%H2	62/50 sccm	60min.

Representative XRD scans for samples ST-1-1 and ST-1-62 are shown in figure 5.10 and 5.9, respectively. The peaks can be indexed to Erbium Chloride Silicate (ECS), Gold and Silicon as labeled. The ECS peaks are well indexed with an orthorhombic crystal with lattice parameters of a= 6.8218 Å, b=17.6519 Å, and c= 6.1601 Å and the peaks are well matched with data (JCPDS card: No. 00-042-0365) for $Er_3Cl(SiO_4)_2$. On the other hand, Si and Au peaks are well indexed with

cubic crystals with lattice parameters a= 5.4309 Å, b= 5.4309 Å, c= 5.4309 Å and

a= 4.0786 Å, b= 4.0786 Å, c= 4.0786 Å, respectively. Those peaks are well

matched with data (JCPDS card: No. 00-027-1402 and 00-004-0784) for Si and

Au. As seen in both scans, the major peak for $Er_3Cl(SiO_4)_2$ is near 30° which

corresponds to the (060) plane of the ECS material. In order to determine the

crystal quality, we should deal with this peak because the growth direction of the

nanowires is in [060] direction which is perpendicular to the (060) plane. The

crystal structure of the ECS material with growth direction is shown in figure 5.7.
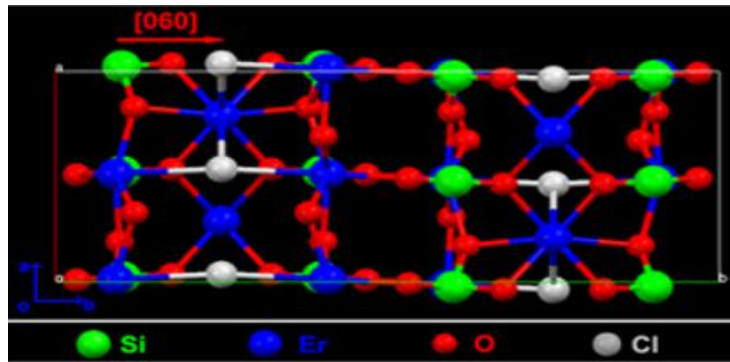
Figure 5.7 The crystal structure of ECS [4]

It is very obvious that there is no any peak matching with Si for the first

sample. However, when we take a look to the second sample, there exist a few

peaks matching with Si pattern. Although there is a huge peak at 56° which

corresponds to Si, it is believed that the signal comes from the substrate because it

is very strong signal compared to the others. However, the peaks at 28° and 47°

belong to the Si core layer. If there is no crystalline Si inside the wire, scan should

not give any signal as happen in ST-1-62 because ECS is a compound material

and the elements inside ECS cannot be evaluated separately. Therefore, this

comparison show us we can grow pure ECS nanowires when the growth

temperature (substrate temperature) is 1070 C. On the other hand, when the growth temperature is 955 C, the product becomes Si/ECS core-shell structure. Meanwhile there are a few peaks which match with Au pattern in the scan of ST-1-1, but those are not observed in another scan. Due to five times thicker gold layer than ST-1-62, existence of those peaks is reasonable in ST-1-1 because thicker layer make the droplets bigger and there exist a big gold particles that can be detected by XRD on the tip of the nanowires. Another important evaluation that we can make from the scans is the sharpness of the peaks. As explained before, the shape of the peaks also give us much information about the crystals. As seen in the scan of ST-1-62, the main peak of the ECS is very sharp and the magnitude of the peak is also very high. Since it is very sharp, FWHM is also very small. In ST-1-1, however, magnitudes of the peaks are very weak and the peaks are very wide compared to the others in ST-1-62. Those are also very important to make comment about the crystalline quality of our nanowires. From those comparison, we can also conclude that higher growth temperature always tend to make our nanowires have better crystalline quality. Since ST-1-62 contains pure ECS nanowires which means there are more Er ions inside the wires and also the FWHM is very small compared to the other, we can estimate that PL emission of sample ST-1-62 should be much stronger than emission of ST-1-1. In order to confirm this, PL measurements for both samples were made and we found out that the integrated intensity for ST-1-62 and ST-1-1 is 150000 and 35000, respectively. So the PL measurements also proved that higher growth temperature makes nanowires give very high luminescence intensity by both

doing crystalline quality better and containing more Er ions. Although we showed two samples to make a comparison here, we actually did many XRD analyses for a number of samples, and another comparison for the samples grown at different growth temperatures is shown in figure 5.8. In this figure, we plot the FWHM of (060) plane versus substrate temperature. Since FWHM is one of the key to determine the crystalline quality, it shows that higher growth temperature makes the samples better in terms of crystalline quality because FWHM gets smaller as the growth temperature increases.
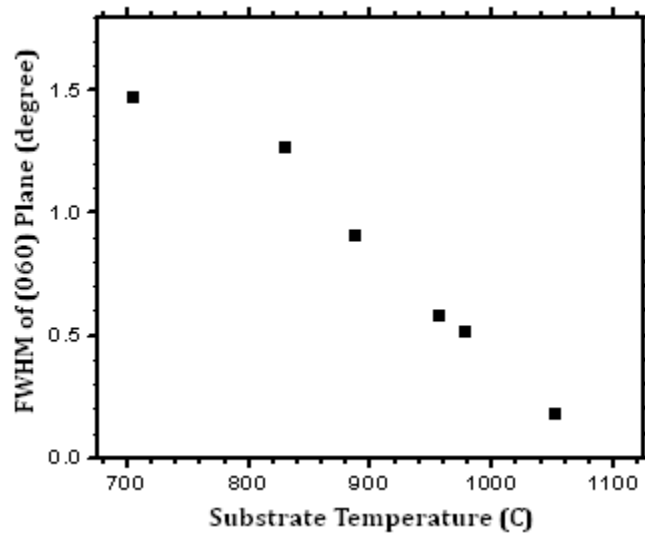
Figure 5.8 Linewidth of (060) plane peak versus Substrate temperature.
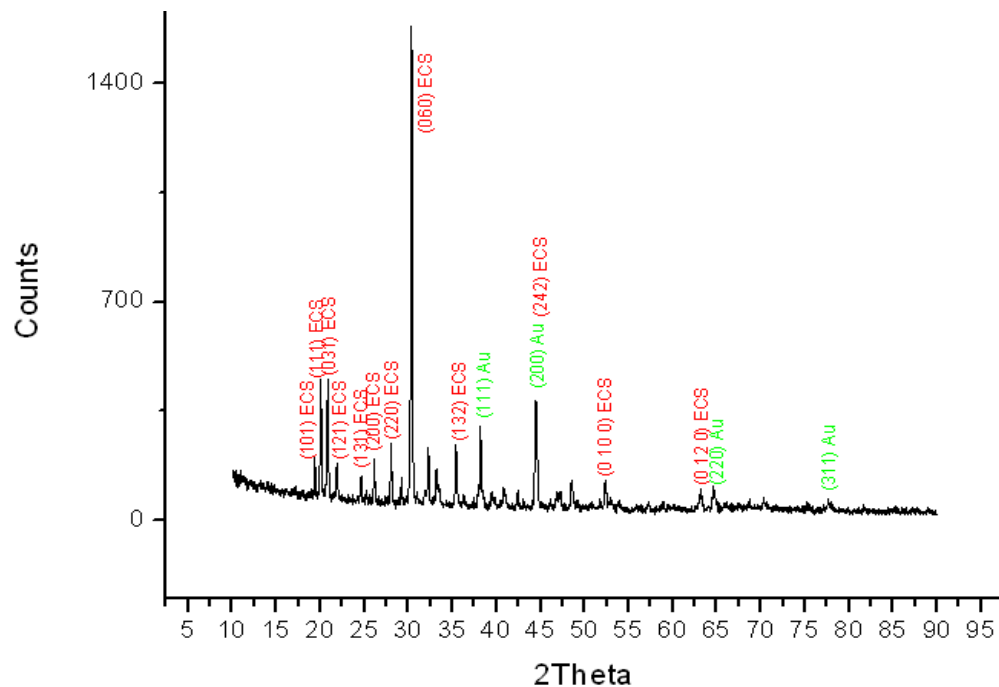
Figure 5.9 XRD spectrum of the sample ST-1-62.
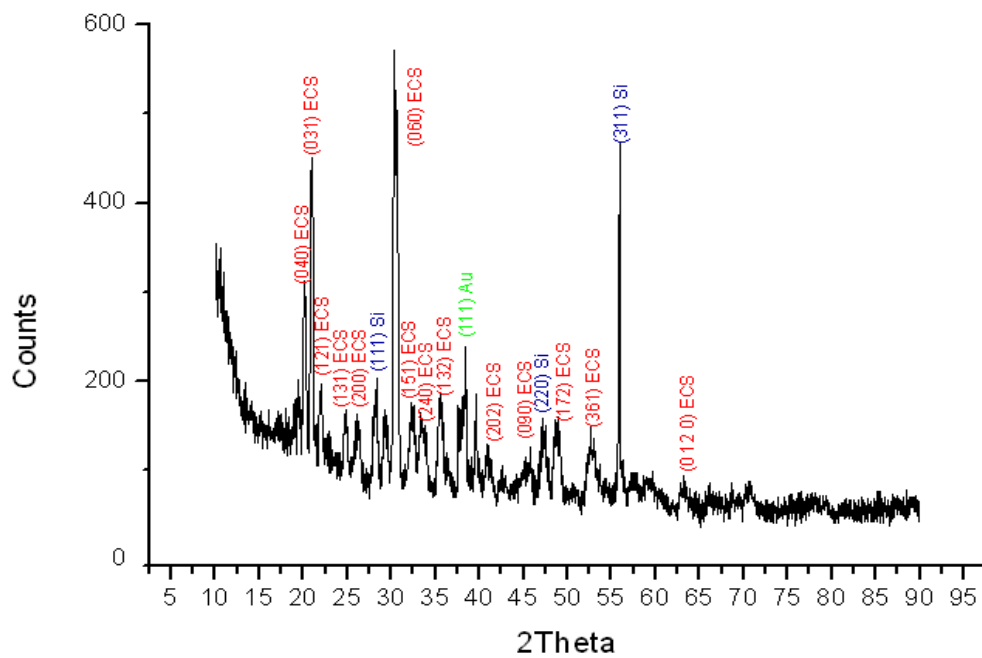
Figure 5.10 XRD spectrum of the sample ST-1-1.

5.5.1 Photoluminescence

PL measurements were carried out using our NIR setup shown earlier and it is found that the major luminescence peak, which corresponds to 1.53 μm, comes from the $^4I_{13/2} \rightarrow {}^4I_{15/2}$ intra-4f states transition of Er ions. Other smaller peaks near the major one come from the sub-bands of the 1st and ground states in a crystal field as explained before. The PL spectrum of one of our samples is shown in figure 5.11 and it gives very sharp lines which indicate the crystal quality is very good. For ECS nanowires, many PL measurements were done from 77K to room temperature and it is found out that when the temperature increases the peaks are broadened, but even at room temperature the separation of the peaks is very good. This also shows how good the crystalline quality of our nanowires is. One of PL measurements done by our group members show that the line width at 77K is only 0.8nm which is much smaller than the other erbium compound materials such as erbium silicate, erbium oxide, and so on. [4] In fact, as we mentioned before, the problem with Er related materials is that high Erbium concentration cannot be achieved effectively in the material. Even if it is achieved in some cases, those Erbium ions will act differently due to high concentration in a crystal field and this makes the line width broad. However, this is not the case for our ECS nanowires owing to its crystal nature.

In result and discussion section, it is indicated that growth temperature changed the crystalline quality of our samples significantly based on XRD scans. It is well known when the crystalline quality is better, photoluminescence
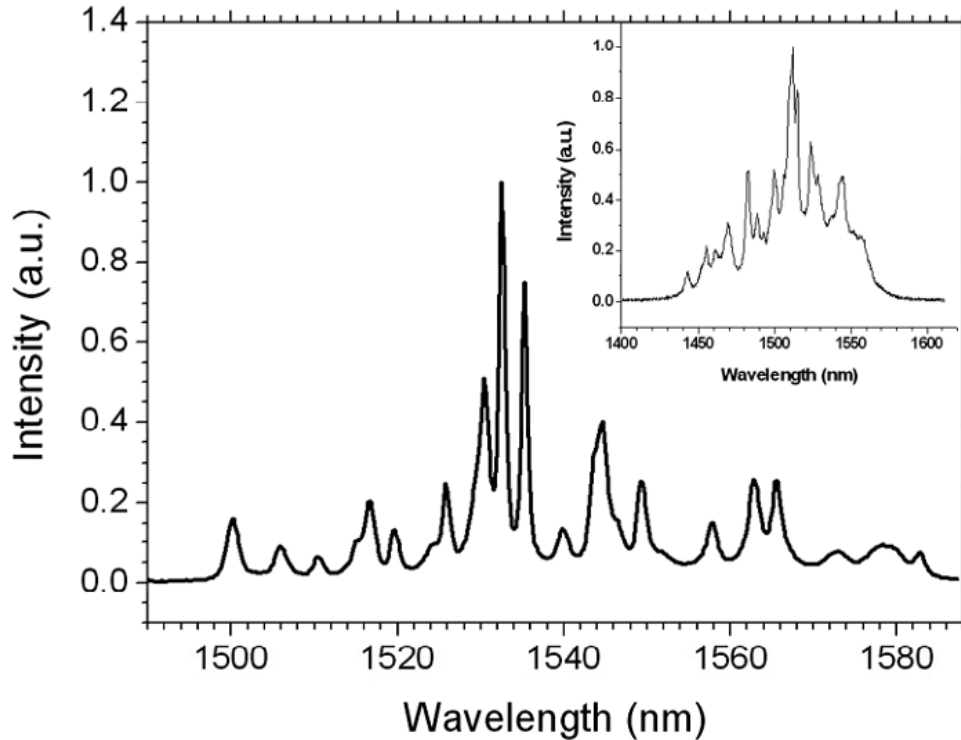
Figure 5.11 Normalized PL spectrums of ECS nanowires at 77K and at the room temperature (inset). FWHM is much narrower at 77K and it gets wider as temperature increases.

peaks become sharper and the intensity of the lines gets larger as explained the cases for ECS material and other Er compound materials. Since the light emission depends on the crystalline quality as well and we got different samples with distinct crystalline quality at different growth temperatures, we did a number of PL measurements for ECS samples grown with the growth temperatures from 910 C to 1050 C to make a comparison between them.

As seen in figure 5.12, the integrated PL intensities increase almost linearly with increasing growth temperature. This also shows that higher growth temperature causes nanowires to have better crystalline quality and give high luminescence intensity. The idea, which I believe make the emission stronger with higher growth temperature, is that Si core is incorporated with Er, Cl and O

and it is completely changed to the ECS material after the incorporation and by
this way nanowires contain more Er ions and the luminescence becomes much
stronger compared to the others grown at low temperature. For low temperature
growths, it has been shown that the structure is Si/ECS core/shell and this kind of
structure does not contain as high as Er ions in pure ECS structure.
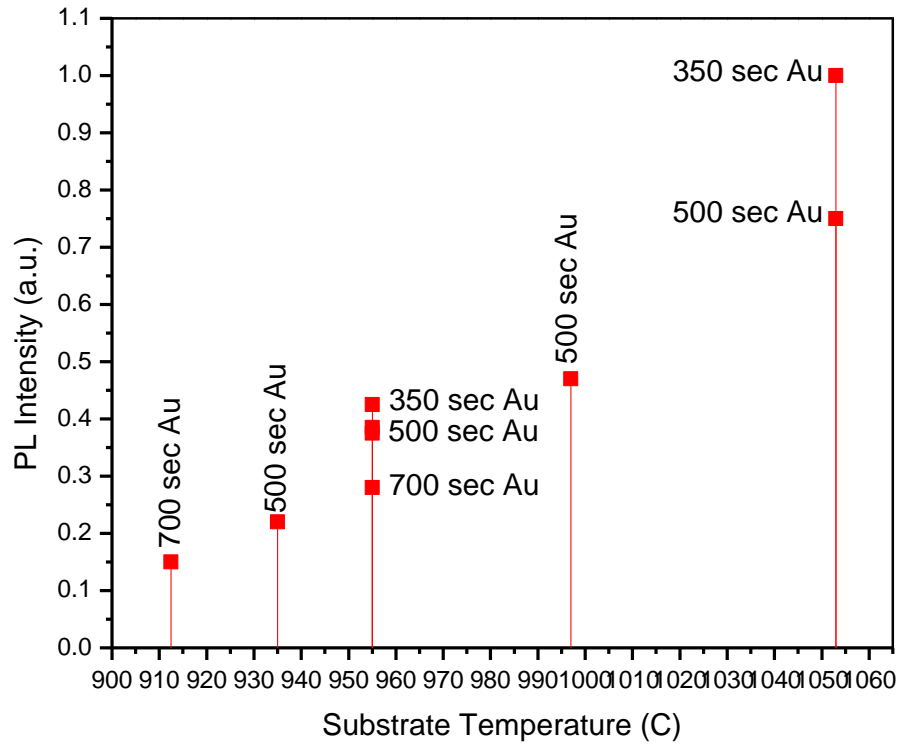
Figure 5.12 Normalized integrated PL intensity versus substrate (growth)
temperature. The labels on squares represent the gold sputtering time onto the
substrate.

For the comparison of PL intensity with the increasing growth
temperature, different gold thicknesses were used to grow nanowires although the
other conditions were almost same. It is very interesting to mention that the
growths at 955 C and 1050 C were performed by using various gold thicknesses
and the result is surprising. We used to believe that when thicker gold layer is

used, the metal droplets can get bigger and we grow wider nanowires which can cause to give higher luminescence. However, this experiment shows that it is not as we think and when the layer gets thicker, this decreases the luminescence intensity. The only reason that we can think for causing this reduction is that since the gold concentration is higher on thicker layer, the possibility of gold diffusion into the wires increases and this reduces the light intensity because gold is a deep level impurity for Si. Actually, our thought should be correct but there must be a limit for the thickness. Since the thickness is much for those cases, intensity is degraded. However, more research should be done to have further information about this and to prove our observations.

5.5.2 The influence of Gold layer thickness

As indicated in the first chapters, the diameter of the nanowires basically depends on the size of metal catalyst. This was illustrated earlier for some samples but those samples were grown in different furnace run. In order to observe the influence of nanowires` size change on the same substrate, we deposited three different regions on a single substrate with different gold thicknesses. The idea beneath it is to have different regions with different gold concentration. For instance, thicker gold layer makes the metal droplets bigger due to high gold concentration. For this particular experiment, we sputtered 100 sec, 200 sec and 300 sec gold onto different regions of the substrate. In other words, 9 nm, 18 nm and 27 nm gold layers were deposited on the $Si/SiO2$ substrate using sputter coater machine and this substrate was used to synthesis

ECS nanowires. The way we applied to sputter different gold layer thicknesses is that covering the regions with aluminum foil for each sputtering and just leaving the corresponding region uncovered. After the growth, sample was examined using XL-30 SEM machine at secondary electron mode.

As seen in figure 5.13, the thicker region has wider nanowires and the thinnest region has the much narrower nanowires compared to the other region as expected. According to this experiment, we can conclude that higher gold concentration forms bigger metal droplets and then nucleation event occurs via those droplets to grow nanowires. However, although wide nanowires can be grown on a region which has high gold concentration, the PL emission is degraded more by thicker gold layers as explained in Photoluminescence section.
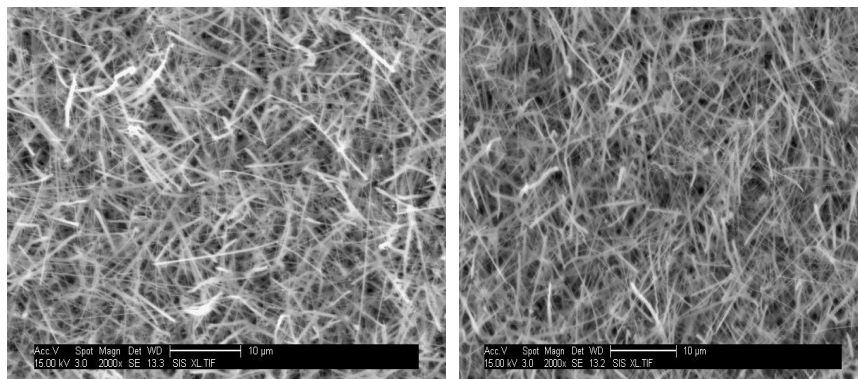
Figure 5.13 SEM images of different regions on a substrate. Left image was taken from the sample grown with 27 nm gold layer and the average diameter of nanowires is 250 nm. On the other hand, the right one was grown with 9nm gold layer on the different region but same substrate, and the average diameter is 150 nm.

5.5.3 Proof of Catalytic Growth

Although we observed gold tips for some of our samples such as ST-1-2 and ST-1-26 as seen in their SEM images (see figure 5.6), we could not see any gold tip for most of the samples. The reason why we could not see the gold tips

can be due to either gold migration as explained in 2.3 or the growth mechanism which is different from VLS or the limits of the SEM machine. In order to prove the growth mechanism, we patterned $Si(100)/SiO_2$ substrate with Au and this patterned substrate was used to grow ECS NWs to see whether the growth mechanism relies on VLS or any other mechanisms. In general, if NWs are grown without pre deposited catalyst which means no metal cluster on the substrate, it does not necessarily mean that NWs are grown without catalyst. In those cases, one of the source materials decomposes and one element of the precursor acts as a catalyst and NW growth is initiated via this native element.

So, to see the case in our ECS nanowire growth, we created 400x200 μm^2 rectangular shape gold patterns with 100 μm spacing between them on the substrate and NWs were grown on this patterned substrate. After the growth had been performed, morphology of the NWs and the surface of the substrate were examined using XL-30 SEM machine. As seen in figure 5.14, the region without Au layer has nothing. On the other hand the patterned regions apparently have products so that this experiment shows us the proof of VLS growth mechanism involved in the ECS NW growth.
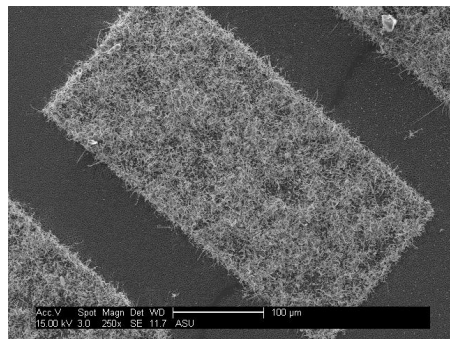
Figure 5.14 SEM image of the patterned substrate after the growth.

5.6 Conclusion

To sum up, we found a new Si based Er compound material in both Si/ECS core/shell and pure ECS forms grown via VLS growth mechanism in CVD system. This new Er compound material contains much more Er ions and the Erbium concentration ($1.6 \times 10^{22} cm^{-3}$) is significantly higher than other Er doped/compound materials. The emission lines are much sharper and the emission strength is higher compared to the other Er related materials. Also, photon lifetime for ECS material is longer than other Er compound materials. We showed that higher growth temperature changes the nanowires from core/shell Si/ECS form to the pure ECS form and makes the products better in terms of crystalline quality and since the crystalline quality gets better, this causes to have better optical properties as well. The strongest emission line for ECS material is at 1.53 μm and thereby the new Si based material is expected to find many applications in optical communication, Si photovoltaic (PV) cells to increase the efficiency due to up and down-conversion process in Er, optical amplifiers and chip-scale photonic systems, and many others.

Chapter 6

TWO SEGMENT CdS-CdSe NANOWIRES AND BELTS

6.1 Introduction to two segment CdS-CdSe growths

In recent years, axial nanowires have driven a lot of interest on them due to superior properties to the planar heterostructures counterpart. Since the diameter of axial heterostructures nanowires are small, nanowire lattice can be easily expanded in radial direction and this can relieve strain between lattice-mismatched materials without necessitating strain-relieving misfit dislocations. So, this allows having very high quality heterointerfaces, at which there are very less misfit dislocations, within axial heterostructure nanowires grown by two different lattice-mismatched materials. Therefore, axial heterstructure nanowires offer a significant advantage over planar or bulk materials. However, there are some challenges for growing straight axial nanowires because chemical potentials and surface energies of the different materials, which involve in axial nanowire growth, are different and the differences can cause to change the growth conditions and directions, and final structure cannot be suitable for device applications. Thus, growing axial nanowires requires very detail research to figure out the best conditions for growing straight axial heterostructure nanowires.

Recently, II-VI materials have attracted a great deal of interest due to their unique properties which can be used for novel optoelectronic devices. Among the others, CdS and CdSe are especially promising for Nanophotonic devices because they are direct band-gap materials and their ternary alloy covers almost the entire visible spectral region. In recent years, many researches have been conducted on

CdS and CdSe nanostructures for exploiting their unique properties and so far, field effect transistors, Nanolasers, and photoconductive sensors, and many others have been reported by using these nanostructures. It is important to note that one of the major papers for CdSSe ternary alloys was published by our group in 2009. In this paper, full composition gradient nanowires on the same substrate was demonstrated using temperature gradient method (TGM) and elemental composition gradient (ECG) together , and this paves the way for highly efficient solar cells and full color displays because the wavelength range of materials covers entire visible spectrum. On the other hand, another group from Hunan University was demonstrated CdSSe nanowires with full composition gradient in a same wire rather than on a same substrate. This is also very promising and can be used for many optical devices such as LEDs, lasers and etc. However, CdS-CdSe axial nanowires with abrupt junction have not been demonstrated up to date. Therefore we aimed to do that and we will study CdS-CdSe axial nanowire growth with very short transition region (close to abrupt) in this section. Why we want to grow this kind of nanowires is because we want to build white light LEDs by mixing red, green and blue colors within the same wire. If the junction between different segments is not abrupt, the emission spectrum becomes broadened and the white light quality becomes worse. However, in order to achieve this, we have to grow red and green segments first and after this, we can add another segment using wide band-gap material such as ZnS to get blue color. Since the first step is very important for our final goal, growing CdS-CdSe axial nanowires will be studied through this chapter.

Although growing axial nanowires looks very easy task, it is actually not for some materials due to the fact that a lot of additional processes involve into the growth. First of all, dominance between VLS and VS mechanism should be arranged accordingly because it determines the final shape of the structure. However, this is not as easy as thought due to different chemical potentials of the CdS and CdSe molecules at different temperature zones. Another major problem is the ion exchange between source materials. This phenomenon has been observed by other groups as well and reported elsewhere. Ion exchange between CdS-CdSe, ZnS-CdS and ZnS-CdSe significantly change the structure in terms of morphologically and optically. In our case, ion exchange between CdS and CdSe has been a main bottleneck for growing CdS-CdSe straight axial nanowires.

6.2 Experimental Section

In order to grow CdS-CdSe two segment structures, we utilized the source moving approach which was first used by Reimers et al. for growing full-composition-graded bulk CdSSe in 1980s [2]. It has been also recently used by Gu et al. to synthesis CdSSe composition graded single NWs [27]. The idea for the approach is very simple but versatile. Although the approaches are similar for those experiments, the aim of each one is different. For our case, the approach was applied to get CdS-CdSe two segment structures without having a long transition region which means two segment were tried to be grown with an abrupt junction. The system used to grow CdS-CdSe products is as same as the system used for ECS nanowires; however, there is an extra quartz tube connected to the main reactor tube for introducing the CdSe source while furnace is running. Also,

65

we have a magnetic rod, step motor and motion controller unlike ECS system. (see figure 6.1) The motor is used to introduce the CdSe source and replace CdS source with CdSe in the quartz tube. By changing the speed of motor from motion controller, we can arrange the time between source transitions and this therefore determines the transition region in a nanowire. Since we want to grow segmented nanowires with an abrupt junction or at least with very small transition region, the motor should be used at very high speeds. The speed of the motor we used can be as high as 3 cm/min.

This setup has also 1.5" wide and 4' long quartz tube inside the three zone furnace and nanowire growth occurs in this tube. As seen in figure 6.1, another quartz tube, mentioned earlier, with the same diameter and length is connected to the main reactor tube via ultratorr union and one ends of these tubes are also connected to the gas cylinder and vacuum pump, respectively, same as in ECS setup. The growth of CdS-CdSe axial nanowires requires multiple steps which make the growth more complex than ECS NW growth, and those will be given as a list below. However, before explaining all the steps, it is very important to mention the set temperatures of the zones. For most of our CdS-CdSe NW experiments, just 3rd zone of the furnace was set and the set value for other two zones were kept at 0C. We also used the ceramic fibers between different zones to
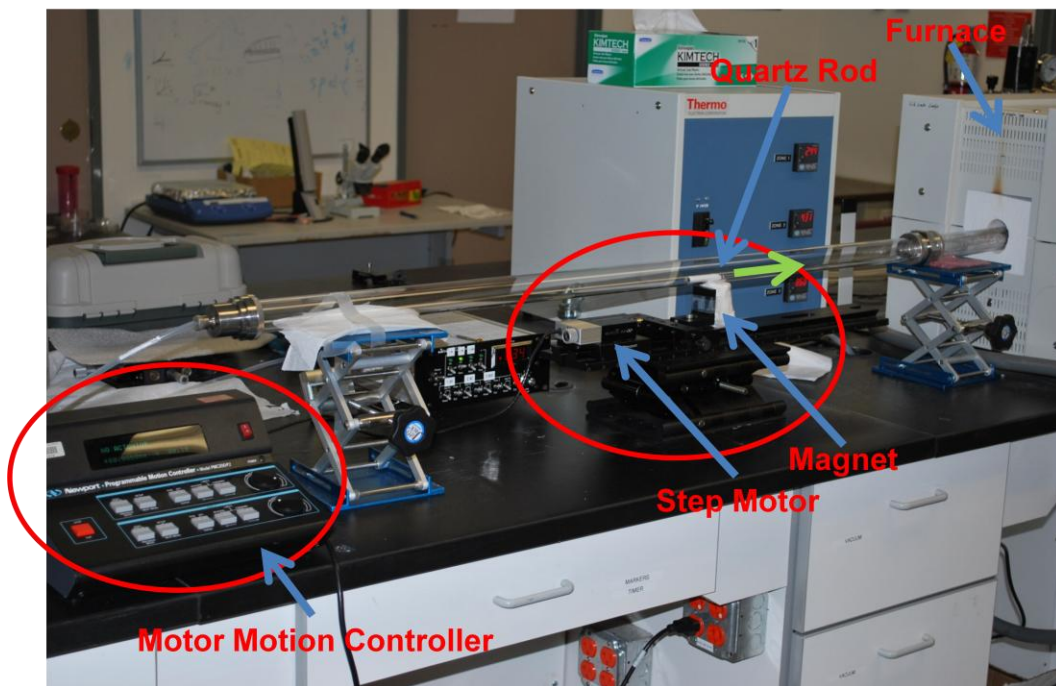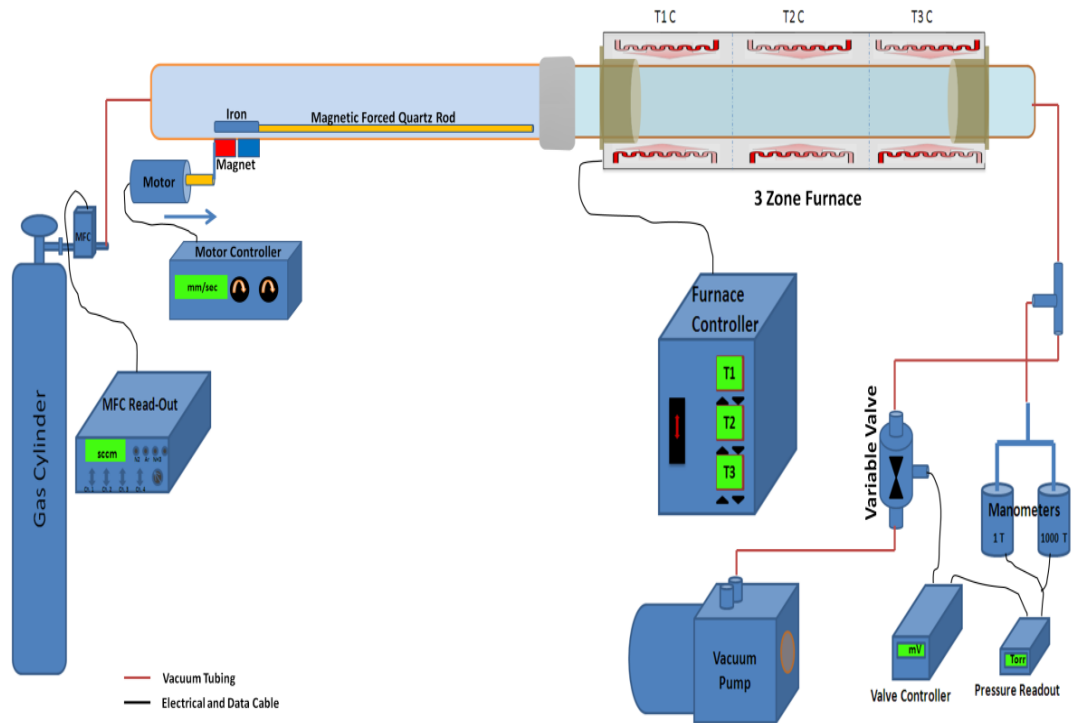
Figure 6.1 Schematic illustration of the system used growing two segment CdS-CdSe structures (a) and real picture of the extension part used for introducing source (b).

isolate the heat inside each zone. Although those zones were set to 0 C, the temperature during the two hours growth can reach up to 550 C in 2nd zone and 350 C in 1st zone due to the heating in the 3rd zone (T3=850 C). However, if ceramic fibers are not used between zones, the temperature in 2nd zone will be very close to the set temperature of the 3rd zone. Therefore, using isolation material is very crucial for having much lower heat inside the adjacent zones. Here, all the steps from 1 to12 will be explained to grow CdS-CdSe two segment structures and the basic schema for the growth configurations is shown in figure 6.2.

1-) Clean the quartz tubes with ethanol and after drying, connect them together with ultratorr union and put the right one into the furnace by allowing 19cm of the tube being outside of the furnace.

2-) Place magnetic rod into the extension tube whose tip will end in the middle of the second zone.

3-) Place CdSe source boat into the center of the second zone-next to the magnetic rod.

4-) Place a 12 cm quartz rod for seperating source boats and CdS source boat from the right end of the reactor tube and push them together via any rod until CdS source boat reaches to the center of the 3rd zone.

5-) Put substrates onto the quartz plate (1.5 cm x 3.7 cm) and place this plate 4-6 cm inside the furnace, depending on the experiment, from the right end. It should be at the middle of the tube and there must be enough space under the plate for shifting the source materials to the outside of the furnace.

6-) Now, all the needs for NW growth were loaded and before turning on and pumping down the furnace, left end and right end should be connected to the gas supply and pump, respectively.

7-) Turn on the mechanical pump to evacuate the system and when the pressure reaches to around 200 mTorr, start checking the system leak rate as explained in ECS NW synthesis.

8-) If the leak rate is fine, open and let the gas flow for a while to flush out oxygen inside the tube and set the variable valve to obtain the desirable pressure in the system.

9-) After the system reaches to the desired pressure, set only the 3rd zone of the furnace and turn it on to start NW growth. (Set temperature varies from 750 C to 900C depending on the experiment.)

10-) Since CdS source is in 3rd zone, the heat applied can evaporate the CdS material and we let the system running for a while for growing pure CdS part.

11-) During pure CdS growth, there is almost no incoming CdSe source vapor toward the substrates because the temperature in second zone is not enough to make it sublimate. After CdS part growth, we use the motor to push quartz rod and therefore the CdSe source as well via magnetic force. The speed is arranged to determine the transition region width. So, the new position of the CdSe source boat is at the center of the 3rd zone where CdS source boat used to be. Since the source boats are shifted together, the new position of the CdS is outside of the

furnace, where the quarzt tube meets with ambient and the temperature is very low, during the CdSe growth part.

12-) After the growth of CdSe part, the furnace is turned off for cooling down. However, there is different options applied during the cooling down process and those are;

a- Keeping CdSe source boat inside the 3rd zone.

b- Pushing CdSe source boat to the outside of the furnace and keeping substrates at their growth position.

c- Pushing CdSe source boat to the outside of the furnace and sliding the quartz tube to the right side to get the position of the substrates out of the furnace which is basically equal with the quenching.

After all those processes are done and waited awhile for cooling, the samples are ready to be checked for their optical and structural properties.
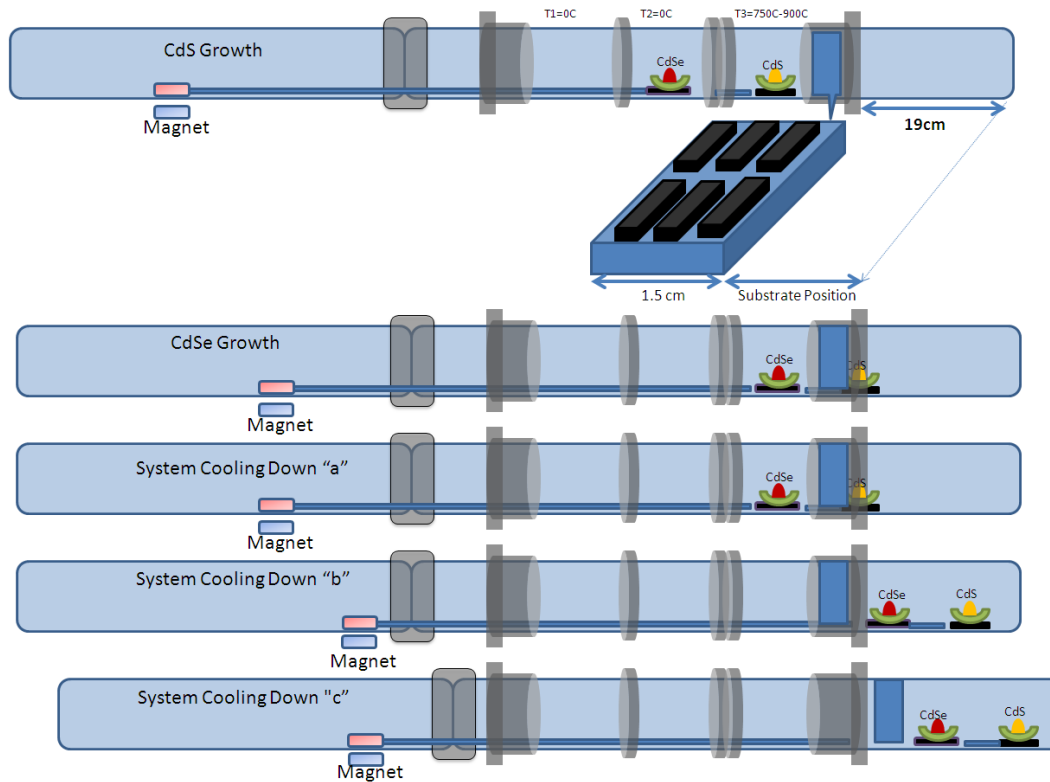
Figure 6.2 Illustration of growth steps for synthesizing two segment CdS-CdSe structures. The sequence flows from top to bottom. Upper configuration is for CdS part growth, the middle one is for CdSe part growth, and the bottom three are for the different cooling down options.

6.3 Characterization Methods

For two segment CdS-CdSe samples, we mostly utilized the photo luminescence measurements to examine the samples. Since we grow segmented structures with CdS and CdSe parts, they look like one piece but they actually have two different segments grown with different materials. The reason why we mostly did PL for those samples is that SEM cannot distinguish the different segments in a structure and it shows the product as a single pure wire or belt. However, due to the fact that different materials emit different color of lights in our case, we can distinguish two different segments from the colors and also morphology can be seen well from the emitting nanowires under dark field optical

71

microscope because the structures are big enough to be seen on the optical microscope. All PL measurements in this section were done using our UV/Visible setup (see Figure 4.2) under 405 nm laser illumination. It is also important to note that most of the PL measurements were done for dispersed nanowires and the process applied to disperse NWs will be explained in the next paragraph. In addition to PL and dark field optical microscope, we also used XL-30 SEM machine on secondary electron mode for some of our samples to see the morphology of the nanowires in detail.

6.3.1 Contact printing

In order to analyze our samples in detail in terms of optical properties, we utilized the contact printing technique. Due to the facts that as grown samples contain high density of nanowires or belts, we cannot make a good optical characterization for those wires. When the density becomes higher, lots of additional effects from other nanowires involve into the emission spectrum; therefore, those make our characterization inaccurate. For example, in case of axial nanowire samples, it is very important to disperse nanowires on another substrate to have sparse nanowires. For our CdS-CdSe growth experiments, it is obvious that there are lots of pure single either CdS or CdSe nanowires although we obtain CdS-CdSe two segment nanowires or belts as well. For this kind of sample, we should have very sparse products to figure out where the emission comes from and by this way, we can analyze even a single nanowire otherwise since the density is very high containing pure CdS, CdSe and CdS-CdSe axial nanowires or core/shell belts, it is not possible to work on the PL spectrum to

figure out the wavelength separations. Therefore we applied contact printing to get sparse nanowires on a new substrate.

The contact printing technique has been developed in recent years and become very attractive because it is very simple but very powerful assembly technique. The detailed contact printing schematic can be found elsewhere [34] and the process is as follows. First of all, the nanowire substrate is bonded to a suitable weight then flipped over the weight and put it on the receiver substrate. The NW donor substrate is at the bottom and the weight on top can provide a suitable pressure. Then the weight and donor substrate are slowly slide over the receiver substrate and the wires will be transferred and aligned on it. The principle under it is the Shear force and it breaks or detaches the wires from the original substrate and the friction between the wire and receiver substrate will align the wires. For better alignment, some lubricant can be added during the sliding process. The lubricant can reduce the friction between the nanowires so that the alignment will be improved and wire stacking will be reduced.

This method is very easy operation, and has good alignment in a large-area. Also the wire density can be very high up to 8 NWs/um. By functionalizing the receiver substrate, the interaction between wire and receiver substrate can be increased and the substrate can grab more wires.

For our experiments, we did not apply the same process explained above. In order to save time and do the optical characterizations quickly for many samples, we just used the following recipe;

1-) Clean a cover glass with Isopropanol which cleans the residues and makes the cover glass suitable to grab more nanowires.

2-) Flip down the donor substrate on a cover glass and apply some pressure and slide the donor substrate on the cover glass via tweezers.

3-) Lift the donor substrate.

After applying these steps which can be also seen in figure 6.3, cover glass will have sparse and aligned nanowires on it and it becomes very suitable to do PL characterization for the nanowires. In case the receiver substrate grabs more nanowires than needed, pressure applied by tweezers should be lowered or the cover glass should be waited longer time after cleaning with Isopropanol. Due to the easiness of the technique, many research groups exploit it for building nanowire based photonic and electronic devices and it seems the usage of this technique will increase in the future without doubt.
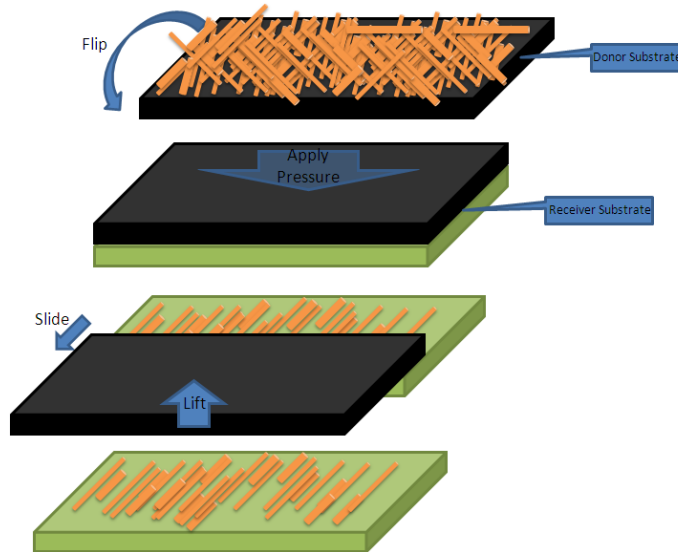
Figure 6.3 Schematic illustration of contact printing method used in the thesis.

6.4 Result and Discussion

Although the aim of this study is to grow straight CdS-CdSe axial nanowires, we have observed that various kinds of structures in different forms, such as nanowire, nanobelts, and flag like, are unintentionally grown. Through this passage, we will discuss all those type of structures by giving examples from our experiments. Before go into that part, it is important to mention that we did a number of experiments to grow pure CdS and CdSe before trying to grow segmented products, and as a result, we found out that the most appropriate pressure for growing pure CdS and CdSe is 225 Torr and the flow rate is around 35 sccm N2. Since that values work well for growing pure CdS and CdSe, we used those also for growing segmented nanowires and nanobelts. Therefore, it can be predicted that all the samples in this part of my research were grown with 30-35 sccm N2 flow under 225 Torr pressure. Dark field optical microscope images show that these grown wires, belts and other structures have the length up to 200 μm and the width is from 100 nm to 1 μm, and SEM images show that these products were grown via Au catalyst because on the tip of the nanowires or belts there is a gold cap. (See figure 6.4) However, the growth mechanism for belt or flag like structures is different because both VLS and VS mechanisms involve in the growth and this will be studied later. Under 405nm laser illumination, there are many products which give two different colors on the sample even though there are some products giving only one single color. From our experiments, different types of structures have been obtained and those are listed in figure 6.5.
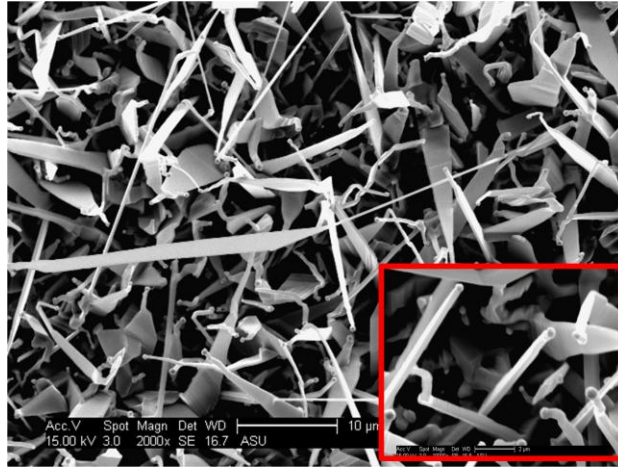
Figure 6.4 SEM image of a CdS-CdSe two segment sample and close up

SEM image (inset).

The types of structures we observed during this research can be listed as

follows and the growth mechanism for each one will be mentioned separately;

- CdS NW + CdSe NW ("a, c, d and f" in figure 6.5)

- CdS NW + transition region + CdSe NW ("b and g" in figure 6.5)

- CdS NW + CdSe Belt ("h" in figure 6.5)

- CdS NW + CdSe NW in flag like structure ("e" in figure 6.5)

- Tapered CdS Belt + CdSe shell layer ("k" in figure 6.5)

- CdS belt + CdSe tapered belt and shell layer over CdS belt ("l" and "m" in figure 6.5)

- CdS sheet + CdSe shell layer ("n and o" in figure 6.5)

- CdS NW + CdS tapered belt with CdSe shell layer in flag like structure ("i and j" in figure 6.5)
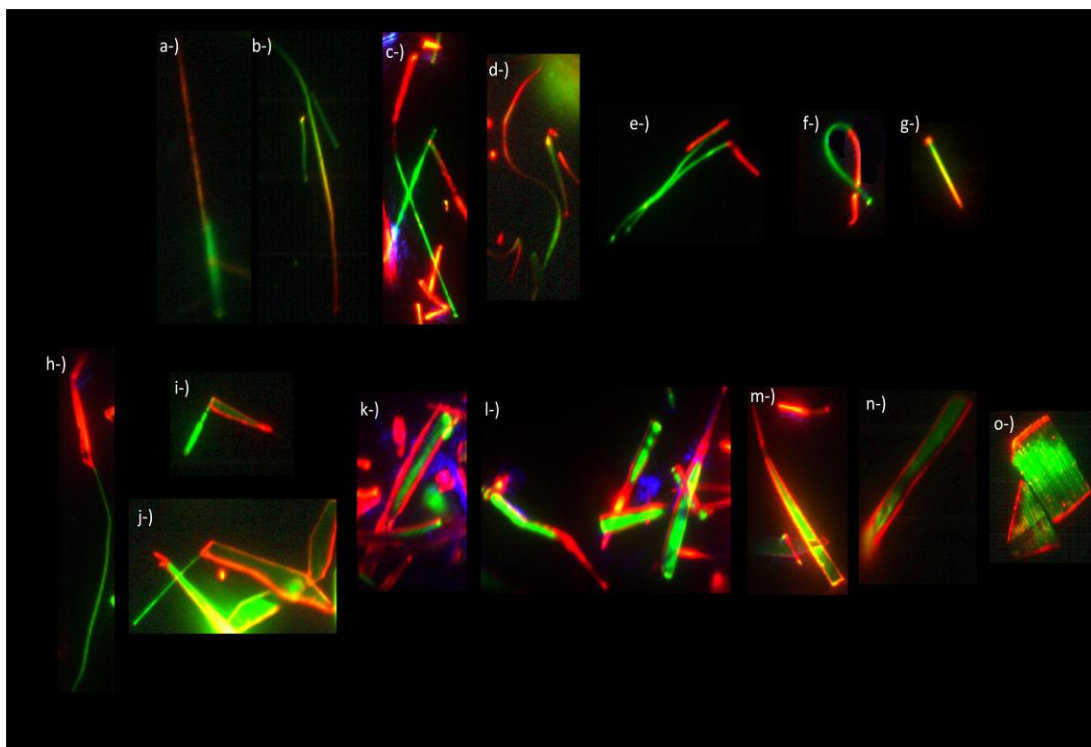
Figure 6.5 PL images of different kinds of structures grown under different conditions. (Each one was addressed in previous page.)

6.4.1 Growing "CdS NW + CdSe NW" type of structure

This type of structure is represented by "a", "c", "d" and "f" in figure 6.5. For some materials, growing straight axial nanowires is very difficult because this type of nanowires requires interfacial surface energy balance. For example, if we want to grow CdSe after CdS part is grown, the sum of surface energy of the Nanoparticles-CdSe and CdSe-CdS should be smaller than the interfacial surface energy of Nanoparticles-CdS. If this is not the case, the product becomes kinked nanowires which mean we can get structure like "e" in figure 6.5. In order to grow this kind of structure, the first think we have to get is the appropriate substrate temperature for the first step of the growth. This can be adjusted by either set temperature or substrate position. If the temperature is low for this step,

product becomes more likely nanowire; otherwise it tends to be nanobelts. After the first step of the growth, source boats are shifted together in two minutes to get abrupt junction, and the CdSe source material, which will be the another part of the nanowire, comes to the center of the 3rd zone. (See figure 6.2) If we keep the source temperature same for CdSe, we have chance to get straight axial nanowires, however, if we shift the substrates little bit downstream where the temperature is lower, we will have more chance to get straight axial nanowires because lower temperature reduces the interfacial energy of Nano particles-CdSe and CdSe-CdS. Therefore, we can satisfy the requirement for the straight axial nanowire growth. Experiment conditions for "a", "c", "d" and "f" in figure 6.5 are listed in table 6.1 just to give some idea how two segment straight axial nanowires can be grown. If those conditions are applied, similar structures can be obtained. However, the emission strength for this type of structures is not very strong due to the low temperature. According to these experiments, low growth temperature makes the crystalline quality bad, and this degrades the emission strength of the nanowires. If the temperature is increased, the structure then becomes different which will be mentioned later.

Table 6.1 Growth Conditions for "CdS NW + CdSe NW" type of structures (See figure 6.5 for the reference. Source positions are as indicated in figure 6.2)

Sample	Pressure (Torr)	N2 Flow (sccm)	Source temp. for CdS/CdSe (C)	Substrate Pos. drng. CdS/CdSe (cm)	Growth Times		
					CdS	Transition	CdSe
a	225	33	865/865	23.3/23.3	2hrs	3min.	7min.
c	225	31	880/880	23/22.5	90min.	3min.	30min.
d	225	33	840/840	25.5/25.5	98min.	2min.	7min.
f	225	31	880/880	23/23	90min.	3min.	30min.

6.4.2 Growing "CdS NW +Transition Region +CdSe NW" type of structure

This type of structure is exemplified by "b" and "g" in figure 6.5. Growing this kind of structure is quite similar with the previous one. However, transition time should be kept longer to get a transition region. Since the time is longer, both sources can be at the high temperature zone at the same time. This basically means there are two active source vapors coming towards the substrates and both can incorporate into the nanoparticles and make alloy. That is why after the green section, we have a yellowish transition region which is the alloy of CdS and CdSe. In the previous case, that time was pretty short and therefore, there was no time which favors for both source materials to incorporate. The growth conditions to grow this kind of structure are indicated in table 6.2 and this is repeatable if similar conditions are applied.

Table 6.2 Growth Conditions for "CdS NW +Transition Region +CdSe NW" type of structures (See figure 6.5 for the reference. Source positions are as indicated in figure 6.2)

Sample	Pressure (Torr)	N2 Flow (sccm)	Source temp. for CdS/CdSe (C)	Substrate Pos. drng. CdS/CdSe (cm)	Growth Times		
					CdS	Transition	CdSe
b	225	33	870/850	23.5/22.5	90min.	6min.	8min.
g	225	33	830/830	22.5/22.5	90min.	8min.	8min.

6.4.3 Growing "CdS NW + CdSe Belt" type of structure

In Figure 6.5, "h" can be given as an example for this type of structure. The first part of this type of structure, which is the CdS NW, can be grown by applying similar conditions used for previous two types. However, the second step of the growth is different because it is belt like structure. In order to grow belt, there is some requirements. First of all, it is known that if the temperature is high, the chance to grow belt increases, but how it happens? In order to grow

79

nanowires, we have to get nucleation at vapor-nanoparticles interface and the nucleation rate depends on the Gibbs-free energy, chemical potential and interfacial surface energy. However, during the growth, nucleation can occur not only on vapor-nanoparticles interface but also vapor-crystal and vapor-crystal-nanoparticles interfaces. If the temperature for the second part of the growth favors the nucleation on both vapor-crystal and vapor-nanoparticles interfaces which basically equal to VS and VLS growth mechanisms, we can get belt like structures. Actually, nucleation at the vapor-nanoparticles interface should not necessarily be occurred to grow belt like structure: however, SEM image shows that this type of structures have a gold cap on the tip which shows nucleation occurred at there. Also, the shape of belt usually becomes tapered and this is because the bottom part of the belt is exposed to supply more time than upper part during the growth and that is why bottom part is wider and top part is narrower. Basically, the growths in axial and lateral directions occur via VLS and VS mechanisms, respectively. Similar structure can be also seen on SEM image in figure 6.4. The growth conditions for this type of structure are shown in table 6.3.

Table 6.3 Growth Conditions for "CdS NW + CdSe Belt" type of structures (See figure 6.5 for the reference. Source positions are as indicated in figure 6.2)

Sample	Pressure (Torr)	N2 Flow (sccm)	Source temp. for CdS/CdSe (C)	Substrate Pos. drng. CdS/CdSe (cm)	Growth Times		
					CdS	Transition	CdSe
h	225	33	850/850	25/25	130min.	3min.	7min.

6.4.4 Growing "CdS NW + CdSe NW" flag type of structure

"E" in figure 6.5 represents this kind of structure. Since the first part of the structure is CdS nanowire, growth conditions of the first stage should be similar with previous ones. The second part is CdSe nanowires; however, the growth direction during the second part of the growth is somehow changed. According to our experiments, this is usually the case when the source and substrate temperatures are decreased. This can be done by decreasing only the source temperature because the substrate temperature is dependent to the source temperature as long as the substrate position is fixed in our system. The mechanism of growing kinked nanowires is related to the interfacial energy balance as mentioned earlier. For this type of structure, the sum of the interfacial energies of Nanoparticles-CdSe and CdSe-CdS is larger than the interfacial energy of Nanoparticles-CdS, and therefore the product becomes kinked because the system wants to make that smaller by changing the growth direction of the second segment. The growth conditions for this particular structure are shown in table 6.4.

Table 6.4 Growth Conditions for "CdS NW + CdSe NW" flag type of structure (See figure 6.5 for the reference. Source positions are as indicated in figure 6.2)

Sample	Pressure (Torr)	N2 Flow (sccm)	Source temp. for CdS/CdSe (C)	Substrate Pos. drng. CdS/CdSe (cm)	Growth Times		
					CdS	Transition	CdSe
e	225	35	880/850	23/23	2hrs.	3min.	32min.

6.4.5 Growing "CdS belt + CdSe tapered belt and shell layer over CdS belt" type of structure

This kind of structure can be represented by "l" and "m" in figure 6.5. The growth mechanism for this particular structure is different than the previous types of structures because both segments are belt in this case. First of all, since the first grown part is CdS belt, the growth conditions should be appropriate for growing belts. The requirements for belt growth were indicated earlier, but just to remind that the growth temperature should be higher than nanowire growth temperature because the nucleation event should occur not only at vapor-nanoparticles interface but also vapor-crystal interface. When the temperature is higher, that reduces the Gibbs free energy at this interface and concentration at this site increases with increasing chemical potential and as a result, nucleation occurs not only in axial direction but also in radial direction. Second step which favors for CdSe growth should be also similar because the second segment is also belt. When we take a look to the image, it is obviously seen that the second segment is more tapered than the CdS part. The reason is that balance between VS and VLS mechanism is better than the first part and the tapered shape is caused by the time difference between upper and bottom part of the CdSe belt under source exposure. However, first segment of the structure, which is CdS belt, was also covered by CdSe during the second stage of the growth. This can happen by diffusion of CdSe molecules to the CdS part or the nucleation event can occur also on the CdS surface during the CdSe growth and this make a shell layer. If the second stage of the growth is kept longer, the CdS belt is bound to be replaced by

82

CdSe molecules which will be explained in the following passage. The growth conditions for this kind of structure are shown in table 6.5.

Table 6.5 Growth Conditions for "CdS belt + CdSe tapered belt and shell layer over CdS belt" flag type of structure (See figure 6.5 for the reference. Source positions are as indicated in figure 6.2)

Sample	Pressure (Torr)	N2 Flow (sccm)	Source temp. for CdS/CdSe (C)	Substrate Pos. drng. CdS/CdSe (cm)	Growth Times		
					CdS	Transition	CdSe
l	225	31	880/880	23.3/23.3	90min.	13min.	14min.
m	225	33	830/830	25	130min.	3min.	7min.

6.4.6 Growing "Tapered CdS Belt + thick CdSe shell layer" type of structure

This type of structure can be presented by "k" in figure 6.5 The idea for creating this kind of structure is very similar with the belt + belt type of structure which was explained in previous passage. However, this is kind of different than other because the growth time of the second segment was kept pretty longer than others. As a result, it has been observed that there is almost no green section on the sample. All the green part, which is the CdS section, was substituted by CdSe molecules. On the PL image, some structures can be seen with green section inside the big belt, but even for those, the covered section is pretty thick. For the other products on the same sample, we can tell that the entire CdS region was almost replaced. This statement first was an assumption for us, but after that, another experiment using exactly the same conditions but shorter CdSe growth part was performed and we figured out that the assumption is a fact. CdSe can easily substitute CdS molecules and the product becomes mostly CdSe and gives only red color. After these experiments, CdSe growth time was started to keep very short to eliminate the substitution process. That is why the growth time for all the CdSe growth sections for experiments mentioned in previous or next

passages were kept very short. In figure 6.6, the difference between longer and shorter CdSe section growths can be apparently seen. In the left image, there is almost no green section for most of the product, but in the right one, we can see that there is a clear CdS belt and it was started to be substituted from one side by CdSe in spite of the short growth time.

Table 6.6 Growth conditions of samples used to show substitution effect. (See figure 6.5 for the reference. Source positions are as indicated in figure 6.2)

Sample	Pressure (Torr)	N2 Flow (sccm)	Source temp. for CdS/CdSe (C)	Substrate Pos. drng. CdS/CdSe (cm)	CdS	Transition	CdSe
k	225	34	880/880	23.5/23.5	80min.	60min.	40min.
l	225	34	880/880	23.5/23.5	90min.	13min.	14min.
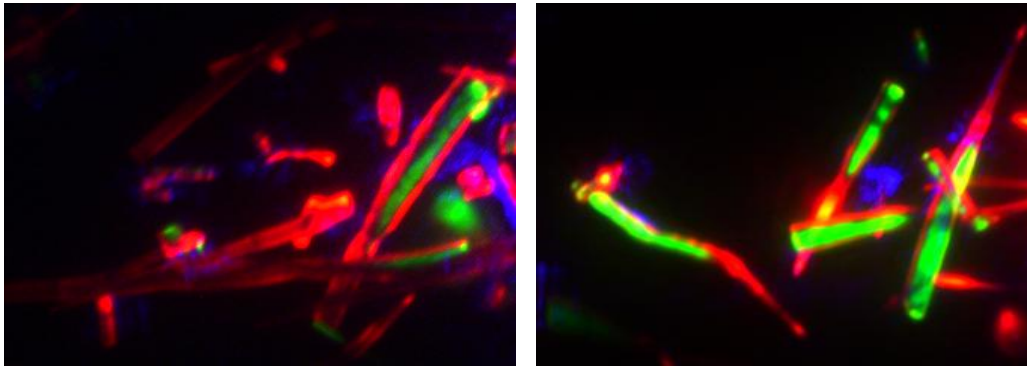
Figure 6.6 Substitution effect on the samples grown with different CdSe growth time. (Left and right images refer "k" and "l" in the table 6.6, respectively.)

As seen in table 6.6, transition time for sample "k" is very long, but there is no transition region in the structure. I think this is not the case for the belt like structure because it is much bigger than nanowire and even if there is this kind of region, this can easily covered and replaced by the subsequent CdSe growth. In the nanowire case, this long transition time creates a transition region in the structure as explained earlier. However, if there is both CdS and CdSe source with enough energy, CdSe becomes always more active and can replace the first grown part. Therefore even for nanowires case, CdSe growth time should be chosen

accordingly. If the CdS part is very long, this does not affect too much but if it is short, then the product can be changed completely.

6.4.7 Growing "CdS sheet + CdSe shell layer" type of structure

As mentioned earlier, VLS and VS growth mechanisms play a very critical role to determine the shape of the structure. If both VLS and VS have the same effectiveness, then the product becomes like tapered belt as shown before. However, if the VS mechanism dominates during the growth, the product becomes a sheet like structure. First, the growth may be start with VLS and creates nanowires, but after temperature reaches to high value, VS mechanism becomes only the active one, and nucleation occur only on the surface of the nanowires and since the growth rate is very high due to high temperature, product becomes like a sheet. For the second step, it is still valid and nucleation continues to occur on this surfaces. In figure 6.5, "n and o" are the examples of this type of structure, but there is a difference between these two samples. We mentioned before that if the growth temperature is high, it favors for growing belt like structure. However, if the temperature is much higher it becomes like sheet which is much bigger than belt because radial growth significantly dominates the axial growth. If the temperature is increased more, then the result will be thin film deposition because the nucleation will occur only between vapor-substrate interfaces via VS mechanism. In table 6.7, the growth conditions are shown, and as seen in the table, the difference between two samples` growth conditions is only the source temperature and this shows that our assumption about the growth mechanism for this type of structure is correct.

85

Table 6.7 Growth Conditions for "CdS sheet + CdSe shell layer" flag type of structure (See figure 6.5 for the reference. Source positions are as indicated in figure 6.2)

Sample	Pressure (Torr)	N2 Flow (sccm)	Source temp. for CdS/CdSe (C)	os. drng. CdS	Growth Times		
					CdS	Transition	CdSe
n	225	33	830/830	26	2hrs.	2min.	8min.
o	225	33	870/870	26	2hrs. 10min.	2min.	5min.

6.4.8 Growing "CdS NW + CdS tapered belt with CdSe shell layer in flag like structure" type of structure

This is very interesting structure and we observed this kind of structure a few times. In figure 6.5, "i and j" are the examples of this kind of structure. Although the growth mechanism is not understood well for this kind of structure, we can just make some comments about it. We believe that the CdS wire part and CdS belt + CdSe shell layer structures are separate in earlier stage of the growth. However, during the growth process, when CdS and another structure get bigger, these two different structures are somehow attached to each other and create this very interesting structure. Otherwise, it is not technically possible to grow this structure because first stage of the growth favors to grow only CdS region and the second stage favors for CdSe. In this structure, there are like three stages which are CdS nanowire, CdS belt and CdSe shell, respectively; however, since the growth conditions changed only once while switching from CdS growth to CdSe growth, the possible mechanism that we thought is the only reasonable one. It is important to note that we can grow belt and nanowires using same material on the same substrate in the same experiment, but there is always one dominant structure such as mostly belt or wire depending on the growth temperature and other

86

conditions. That is why getting CdS wire + CdS belt with CdSe shell layer is possible but the chance is not very high. As a matter of fact, the growth conditions for growing sample i and j are very similar and the products are also very similar. That repeatability makes us think about the other growth mechanisms because for all the other experiments, we have not observed this kind of structure although the possibility of attaching two different structures is high due to the high density. Therefore, more research and experiments on this type of structure should be conducted for further understanding. The growth conditions for these two experiments are shown in table 6.8.

Table 6.8 Growth Conditions for "CdS NW + CdS tapered belt with CdSe shell layer in flag like structure" (See figure 6.5 for the reference. Source positions are as indicated in figure 6.2)

Sample	Pressure (Torr)	N2 Flow (sccm)	Source temp. for CdS/CdSe (C)	Substrate Pos. drng. CdS/CdSe (cm)	CdS	Transition	CdSe
					Growth Times		
i	225	33	840/840	25/25	125min.	2min.	7min.
j	225	33	840/840	25.5/25.5	98min.	2min.	7min.

6.4.9 Comparison of four sequent substrates grown in a same experiment

As illustrated before, the growth temperature is the key parameter to get various kinds of structures for CdS-CdSe two segment experiments. The growth temperature change can be done by either varying source temperature or shifting substrates as explained earlier. In order to observe and prove this temperature effectiveness on the different substrates, we run an experiment using four sequent substrates next to each other with 3mm separation. The idea to put them in a sequence is to get temperature gradient and by this way, each substrate has distinct temperature and the temperature difference between first and last

substrates is around 100 C. The growth conditions for this experiment are listed in Table 6.8 and the growth steps are shown in Figure 6.2. In order to observe the differences between substrates in terms of optical quality and to learn the wavelength separations, we did PL measurement using our UV/Visible PL setup. The PL images were also taken from these substrates to make comments for the morphology of the structures.
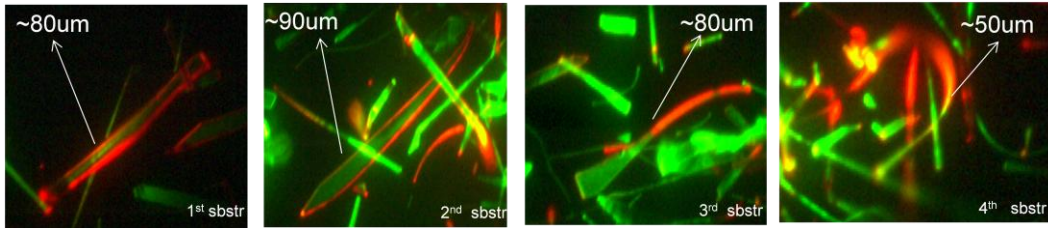

Figure 6.7 PL images of the four sequent substrates.

As seen in figure 6.7, dominance of VLS and VS can be apparently distinguished. The substrate temperature from 1st substrate to last one decreases with a rate of 50 C/cm. Since the first substrate at the higher temperature region, the product is a belt and this shows the VS mechanism dominates in this case. By going further lower temperature region, we can see that VLS growth mechanism becomes the dominant one. 3rd image shows that the growth conditions at this region favor for CdS belt growth but CdSe section becomes nanowire. On the other hand, 4th image shows that the growth conditions at this particular region favors both CdS and CdSe nanowire growths and these conditions meet the interfacial energy balance, hence product becomes like axial two segment nanowire. Figure 6.8 shows the PL characteristics of these samples. Optical quality of the first sample is much better than others and it emits quite strong lights at 546nm and 662nm. The red peak which corresponds to 662nm is stronger

than the green peak despite very small CdSe growth time. When the temperature decreases, CdSe becomes less effective and not only second peak on the spectrum but also first peak, corresponding CdS section, shifts to the left side. In addition, PL emission strength gets weaker by going to the lower temperature zone. So, there is a trade off here if we want to grow product with high PL intensity, that is possible but product becomes belt. On the other hand, if we want to grow straight axial two segment nanowires, that is also possible, but the PL emission becomes very weak. This is very general phenomenon learned from all experiments. Also, the color of deposition on these four substrates changes from red to yellow which shows that the region for CdS deposition is much larger than CdSe and therefore we do not observe red peak for the last sample.
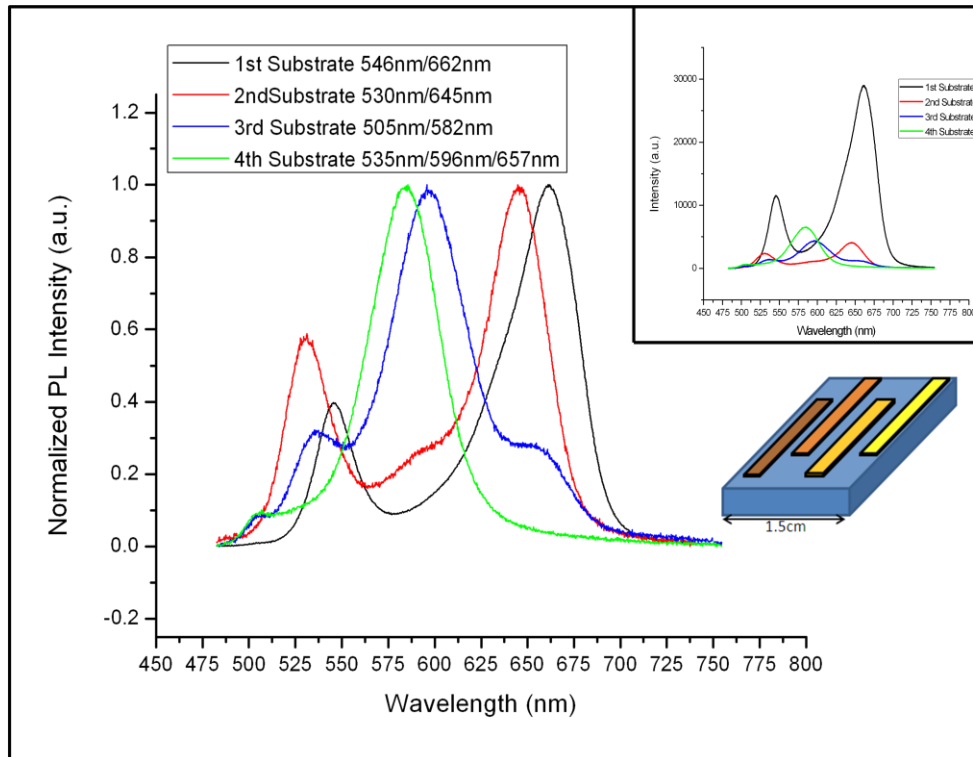

Figure 6.8 Normalized PL spectrums and original spectrums (inset) taken from four sequent substrates of sample ST-3-21. Sequent substrates were put on the quartz plate as seen in the image.

89

6.5 Observations from the two segment growth experiments

Before growing two segment CdS-CdSe, both pure CdS and CdSe nanowires and belts were grown and result shows that the growth range for CdS nanowires is very wide, and we can grow very long (~300μm) pure CdS nanowires using very different conditions. On the other hand, we figured out that this is not the case for pure CdSe growths. The range for growing pure CdSe nanowires is very narrow and it is hard to get caught, therefore the products become usually belt for pure CdSe growths. However, with very detail analyses, it is possible to grow two segment CdS-CdSe nanowires as we reported earlier. For the two segment growths, long CdS section can be grown, but when CdSe source is introduced and becomes active, CdSe molecules replace CdS molecules and this reduces the product length. In addition, pre grown CdS nanowires can be completely changed by CdSe and become single color alloyed nanowires if the CdSe growth is kept longer. This substitution process is very effective for belt like structures as well. As shown before, if we keep CdSe growth time very long, product becomes single color belt; otherwise, we can get a green section inside the core/shell belt structure. Due to these facts, CdSe growth time should be kept very short. Although the CdSe growth time is very short (~5min) compared to CdS growth time (~2hours) for most of the experiments, emission strength from the peak corresponds to CdSe section is very strong. However, this depends also the growth setup. As seen in Figure 6.2, there are three different cooling down options. By applying these three, we can get different results in terms of the emission strength. We figured out that if option "a" is used, the PL emission

90

becomes very weak. The reason can be explained as follows. If there is CdSe source inside the furnace during the cool down process, some CdSe molecules attaches to the surface of the product, but since these molecules have no enough energy due to low temperature, these cannot incorporate into the crystal, and therefore, this degrades the optical quality of the product. However, if the second option called "b" is used, then the emissions from these products become very strong. Another option "c" can be also used to get good emission, but this one also minimize the time spent for cooling down process which is sometimes very valuable for doing many experiments in a limited time. However, we usually used the second option "b" for this research. According to our experiments, we also found out that higher growth temperature favors for better optical quality and the emission strength from products become stronger compared to lower temperature growths. However, there is a trade off here when we increases growth temperature, products become more likely belts and those give strong PL emission, and when we decreases growth temperature, products become more likely nanowires, but emissions from those nanowires become very dim. Since for those experiments Nitrogen was used as a carrier gas, Oxygen molecules inside the reactor could not be flushed out completely and this can cause to have some oxide states in the product. However, since belts are much larger than wires, these states do not affect too many the products and emissions become much stronger than emissions from nanowires. Maybe this problem can be accomplished by using $Ar+5\%H_2$, and by this way, Hydrogen can react with Oxygen, and water vapor can be pumped out via vacuum pump.

Another observation is that if the temperature is decreased during the CdSe growth, this decreases the chemical potential of the CdSe molecules and green section`s emission gets closer to pure CdS band-edge emission, products become more likely straight axial nanowires in case of NW-NW experiments and the wavelength separation gets larger. The max wavelength separation obtained from two segment CdS-CdSe samples is around 160 nm (520 nm-680 nm) and this was obtained when the growth temperature for CdSe section was decreased. It is also very important to mention that if there is both CdS and CdSe sources in the furnace during the CdSe growth, it is not possible to get two peaks corresponding green and red parts of the spectrum; however, it is possible to get greenish and yellow colors even if the CdS source temperature is low during the CdSe growth. That is why we always pushed the CdS source boat downstream of the substrate, and by this way, even if the temperature at this region make it evaporate, that is not very effective and the most important thing is that CdS vapor cannot come to the backward where there are substrates, and the all vaporized CdS source is pumped out.

Very recently, we have also observed two colors lasing from "CdS sheet + CdSe shell" type of structure ("o" in figure 6.5) under high optical pumping power. This type of structure is very suitable for lasing applications because both red and green parts have a medium where gain can occur. However, other types of structures are not suitable for two colors lasing because green part cannot have enough gain due to the red part. Since the energy of green light is higher than the energy of red light, red segment always absorbs the green light, and green light

rays, therefore, cannot go back and forth in the cavity to have population inversion. However, these sorts of structures can also lase by manipulating the structures. Our group is currently working on this type of lasing applications which can be used for novel optical and photonics devices in the future.

6.5.1 The edge effect

We have observed a common phenomenon occurs in most cases of nanowire growths and it is called edge effect. When a substrate is put parallel to the quartz tube plane during the growth, we observe that there are always longer products on the edge of the substrate than other regions on the same substrate. In addition to this, deposition rate on the downstream region of the substrate is much lesser than the upstream region. The reason can be explained as follows. Since the source vapor with high concentration comes to the edge of the substrate first, nucleation event occurs on the edge and starts to grow nanowires or nanobelts earlier than other regions. The remaining source vapor after absorbed by the edge can be used to nucleate nanowires on the other region of the substrate. However, when products get bigger especially at the edge because vapor concentration is more intense there, the other regions are blocked by these long nanowires or belts so that rest of the substrate cannot be supplied with enough source vapors and the unabsorbed source vapor is somehow pumped out from near the substrate or deposited on the quartz tube. In order to eliminate the edge effect in our experiments, we used 10° tilted substrate to the horizontal plane. By this way, we can exploit from the all source vapor coming towards the substrate. Since the level difference between front and back edge of the substrate is more than lengths

93

of the front edge nanowires or belts, back regions can easily absorb the source

vapor. Therefore deposition rate becomes very similar on all over the substrate

and products become uniform. In Figure 6.9, it is illustrated and the deposition

rate differences on the substrates with and without tilting can be apparently seen.
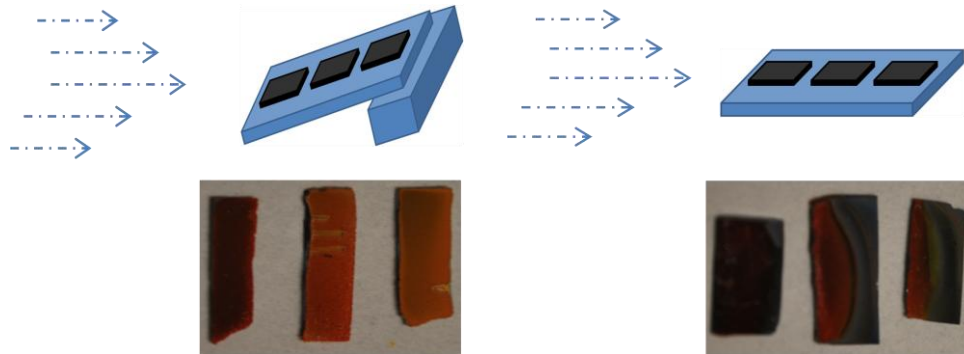

Figure 6.9 10° tilted (left) and parallel (right) substrates to the horizontal plane and their final pictures after growth. Substrates are on a quartz plate. Dashed lines represent the source vapor. The difference between substrate colors is because different growth temperature prefers different composition gradient. The sequence is from the CdSe reach to the CdS reach sample in the real images.
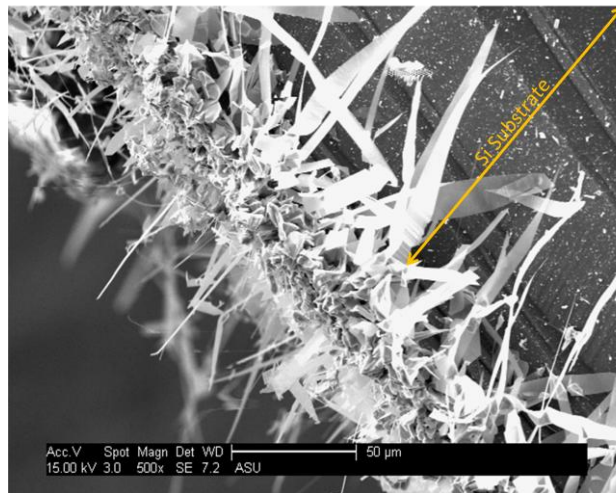

Figure 6.10 Cross sectional SEM image of a two segment CdS-CdSe sample. Since belts, tilted to the right side on the image, are much bigger than other structures, they can easily block the some part of the substrate.

Chapter 7

CONCLUSIONS AND FUTURE WORK

7.1 Conclusions

In the first part of my research, we demonstrated the growth of very new material, which is called Erbium Chloride Silicate (ECS), using chemical vapor deposition (CVD) system. Our experiments show that both Si/ECS core/shell and pure ECS nanowires can be synthesized using different growth parameters and those nanowires have very good features. We showed that Erbium concentration in the ECS compound is $1.6 \times 10^{22} \, cm^{-3}$ which is much higher than any other Er compound materials such as Erbium Silicate (ES) and Erbium oxide. This is a very good improvement because Si is not a good host material and the concentration of Er is usually under $10^{22} \, cm^{-3}$ for Er compounds. Therefore, this material promises to get enough gain and use it as a Si base light source at 1.53um which is in the lowest loss window for fiber optic communication. Furthermore, photoluminescence (PL) emission lines of ECS are sharper and stronger than other Er-related materials which show that they have very good optical and crystalline quality; as well as we demonstrated that those lines in both PL and XRD spectrums get narrower and stronger as the growth temperature increases. This new material can be used not only for Si based LED devices but also amplifiers and solar cells.

In the second part, we demonstrated the growth and characterization of CdS-CdSe two segmented nanowires and belts. Since our final goal is creating white light LEDs using a single nanowire which contains three different segments

95

with the color of red, green and blue, we divided this into two parts. The first part is to create only CdS and CdSe segments in a same structure, and the second step is to add wide band-gap material such as ZnS to get another segment which gives blue light. Since the band-gap energy of CdS and CdSe is 2.42 eV and 1.73 eV, respectively, we are able to get red and green luminescence from those materials. However, the growth of these two materials into a single wire or belt was not as easy as the technique used for simple axial nanowire growths because lots of additional issues such as dominance of VS over VLS and ion exchange processes between CdS and CdSe have involved into the growth procedure. Therefore, very detail research and many experiments were required to catch the most appropriate fashions to grow two segment nanowires and belts successfully using these materials. In this work, we grew good nanowires and belts in different forms and those show spontaneous emission at two different wavelengths under 405nm optical excitation and the separation of these two wavelengths can reach up to 160nm depending on the growth conditions. Also, we demonstrated that belt like structures grown in this study show two wavelengths lasing at the same time when the optical pumping power is high. So, this type of products can have a great deal of interest to use them for creating novel optical and photonic devices.

7.2 Future Work

Due to the fact that our aim for doing the CdS-CdSe growth first is to build white light LEDs using single nanowires which give three different colors, one of my next works will be the growth of ZnS-CdS-CdSe axial three segments nanowires and their optical and structural characterizations.

Another work will be the growth of InGaN full composition gradient nanowires on the same substrate utilizing elemental composition gradient and temperature gradient methods using halide chemical vapor deposition (HCVD) technique. We actually initiated this research before but we had to delay this due to another projects. If we success this, it would be great for many device applications because InGaN can cover the spectral region from UV to IR which is very valuable feature for solar cells. Also, these materials are much more stable in terms of mechanically and chemically compared to the others and the mobility is also very high to use them for high speed devices. After the growth of full composition gradient nanowires on the same substrate is achieved, we can also try to grow axial segmented nanowires as in the case of CdS-CdSe using InN, GaN and their ternary alloys to make white light LEDs or lasers.

Beside nanowire synthesis and the structural characterization, I also plan to involve more into the optical characterization part of the samples and into the fabrication process of devices using our samples.

REFERENCES

[1] R. S. Wagner and W. C. Ellis, "Vapor-solid-liquid mechanism of single crystal growth", Appl. Phys. Lett. 4, 89 (1964)

[2] (a) Reimers, P, Ruppel,W. Phys. Status Solidi B 29, K31 (1968)
    (b) Reimers, P. Phys. Status Solidi B 35, 707 (1969)

[3] Bahram Jalali, "Silicon Photonics", Lightwave Technology 24, 12 4600-4615 (2006)

[4] A. L. Pan, L. Yin, Z. Liu, M. Sun, P. L. Nichols, R. Liu, Y. Wang and C. Z. Ning, "Single-crystal erbium chloride silicate nanowires as a Si-compatible light emission material in communication wavelength", Opt. Mater. Express. **1**, 1202 (2011).

[5] C. T. Huang, C. L. Hsin, K. W. Huang, C. Y. Lee, P. H. Yeh, "Er-doped silicon nanowires with 1.54m light-emitting and enhanced electrical and field emission properties",Appl. Phys. Lett. 91, 093133 (2007)

[6] Erbium Doping in Silicon Nanocrystal, (http://nanoelectromohib.wordpress.com)

[7] Polman, J. S. Custer, E. Snoeks, and G. N. van den Hoven , "Incorporation of high concentrations of erbium in crystal silicon",Appl. Phys. Lett. 62, 507 (1993)

[8] Miritello et al., "Efficient Luminescence and Energy Transfer in Erbium SilicateThin Films", Adv. Mater. 19, 1582–1588 (2007)

[9] V. Yu. Timoshenko, O. A. Shalygina, M. G. Lisachenko, D. M. Zhigunov, S. A. Teterukov, P. K. Kashkarov, D. Kovalev, M. Zacharias, K. Imakita, and M. Fujii, "Erbium Ion Luminescence of Silicon Nanocrystal Layers in a Silicon Dioxide Matrix Measured under Strong Optical Excitation" ,Physics of the Solid State 47, 1, 121–124 (2005)

[10] Zheng et al., "Room-temperature sharp line electroluminescence at X=1.54 pm from an erbium-doped, silicon light-emitting diode", Appl. Phys. Lett. 64 (21), (1994)

[11] Lingling Ren, Won-Young Jeung, Hee-Chul Han, Kiseok Suh, Jung H. Shin and Heon-Jin Choi, "Optical activation of Si nanowires by Er3+ doped binary Si–Al oxides films derived from sol–gel solutions", Optical Materials 30, 497–501 (2007)

[12] Y. Yin et al., "1.53 μm photo- and electroluminescence from Er3+ in erbium silicate", J. Phys.: Condens. Matter 21, 012204 (4pp) (2009)

[13] Daniel E. Perea, Nan Li, Robert M. Dickerson, Amit Misra, and S. T. Picraux, "Controlling Heterojunction Abruptness in VLS-Grown Semiconductor Nanowires via in situ Catalyst Alloying", Nano Lett.11, 3117–3122 (2011)

[14] Wei Lu and Charles M Lieber, "Semiconductor nanowires", J. Phys. D: Appl. Phys. 39, R387–R406 (2006)

[15] Yat Li, Fang Qian, Jie Xiang, and Charles M. Lieber, "Nanowire electronic and optoelectronic devices", Matt.Today 9, 10 (2006)

[16] S.T. Lee, N. Wang, and C.S. Lee, "Semiconductor nanowires: synthesis, structure and properties", Materials Science and Engineering A286, 16–23 (2000)

[17] Xia et al, "One-Dimensional Nanostructures: Syntheses, Characterization and Applications", Adv. Matter. 15, 5 (2003)

[18] Peidong Yang, Ruoxue Yan, and Melissa Fardy, "Semiconductor Nanowire: What's Next?" Nano Lett. 10, 1529–1536 (2010)

[19] Christopher Ma, Daniel Moore, Yong Ding, Jing Li and Zhong Lin Wang "Nanobelt and nanosaw structures of II-VI semiconductors", Int. J. Nanotechnology 1, 4 (2004)

[20] Joyce et al., "III–V semiconductor nanowires for optoelectronic device applications", Progress in Quantum Electronics 35, 23–75 (2011)

[21] Wacaser et al., "Preferential Interface Nucleation: An Expansion of the VLS Growth Mechanism for Nanowires", Adv. Mater. 21, 153–165 (2009)

[22] Kimberly A. Dick, "A review of nanowire growth promoted by alloys and non-alloying elements with emphasis on Au-assisted III-V nanowires", Progress in Crystal Growth and Characterization of Materials 54, 138 173 (2008)

[23] Dick et al., "The Morphology of Axial and Branched Nanowire Heterostructures", Nano Letters 7, 6 1817-1822 (2007)

[24] Paladugu et al., "Novel Growth Phenomena Observed in Axial InAs/GaAs Nanowire Heterostructures**", Small 3, 11 1873 – 1877 (2007)

[25] Kim et al., "CdS/CdSe lateral heterostructure nanobelts by a two-step physical vapor transport method", Nanotechnology 21, 145602 (5pp) (2010)

[26] Shadi A. Dayeh, Robert M. Dickerson, and S. Thomas Picraux, "Axial bandgap engineering in germanium-silicon heterostructured nanowires", APPLIED PHYSICS LETTERS 99, 113105 (2011)

[27] Fuxing Gu, Zongyin Yang, Huakang Yu, Jinyou Xu, Pan Wang, Limin Tong, and Anlian Pan, "Spatial Bandgap Engineering along Single Alloy Nanowires", J. Am. Chem. Soc. 133, 2037–2039 (2011)

[28] Yang et al.,"On-Nanowire Spatial Band Gap Design for White Light Emission", Nano Lett. 11, 5085–5089 (2011)

[29] Xiujuan Zhuang, C.Z. Ning, and Anlian Pan, "Composition and Bandgap-Graded Semiconductor Alloy Nanowires", Adv. Mater. XX,1–21 (2011)

[30] Christopher Ma and Zhong Lin Wang, "Road Map for the Controlled Synthesis of CdSe Nanowires, Nanobelts, and Nanosaws a Step Towards Nanomanufacturing", Adv. Mater. 17, 1–6 (2005)

[31] "Semiconductor Material and Device Characterization" by Dieter K. Schroder

[32] Dissertation "Optical and Crystal Structure Characterizations of Nanowires for Infrared Applications" by Minghua Sun

[33] C. Z. Ning, "Semiconductor nanolasers", Phys. Status Solidi B 247, 4 774–788 (2010)

[34] Z. Fan et al., "Wafer-Scale Assembly of Highly Ordered Semiconductor Nanowire Arrays by Contact Printing", Nano Lett. 8, 20 (2008)

[35] ANDREA R. TAO, JIAXING HUANG, AND PEIDONG YANG, "Langmuir Blodgettry of Nanocrystals and Nanowires", ACCOUNTS OF CHEMICAL RESEARCH 41, 12 1662-1673 (2008)

[36] Hideo ISSHIKI and Tadamasa KIMURA, "Toward Small SizeWaveguide Amplifiers Based on Erbium Silicate for Silicon Photonics", IEICE TRANS. ELECTRON., E91−C, .2 (2008)

[37] Volker Schmidt and Ulrich Gösele, "How Nanowires Grow", Science 316, 698 (2007)

[38] J. B. Hannon, S. Kodambaka, F. M. Ross and R. M. Tromp, "The influence of the surface migration of gold on the growth of silicon nanowires", Nature Letter 10, 1038 (**2006**)

[39] Qian et al., "Gallium Nitride-Based Nanowire Radial Heterostructures for Nanophotonics", Nano Letters 4, 10 1975-1979 (2004)

[40] Dissertation, "Optical and Crystal Structure Characterizations of Nanowires for Infrared Applications" by Minghua Sun